



# Isotope (Sr, C) and U–Pb SHRIMP zircon geochronology of marble-bearing sedimentary series in the Eastern Sierras Pampeanas, Argentina. Constraining the SW Gondwana margin in Ediacaran to early Cambrian times

Juan A. Murra<sup>a,\*</sup>, Cesar Casquet<sup>b,c</sup>, Francisco Locati<sup>a</sup>, Carmen Galindo<sup>b,c</sup>, Edgardo G. Baldo<sup>a</sup>, Robert J. Pankhurst<sup>d</sup>, Carlos W. Rapela<sup>e</sup>

<sup>a</sup> Centro de Investigaciones en Ciencias de la Tierra (CICTERRA), CONICET, Universidad Nacional de Córdoba, X5016GCA Córdoba, Argentina

<sup>b</sup> Departamento de Petrología y Geoquímica, Universidad Complutense, 28040 Madrid, Spain

<sup>c</sup> Instituto de Geociencias (IGEO), CSIC, UCM, 28040 Madrid, Spain

<sup>d</sup> Visiting Research Associate, British Geological Survey, Keyworth, Nottingham NG12 5GG, UK

<sup>e</sup> Centro de Investigaciones Geológicas, CONICET, Universidad Nacional de la Plata, 1900 La Plata, Argentina

## ARTICLE INFO

### Article history:

Received 16 October 2015

Revised 5 May 2016

Accepted 6 June 2016

Available online 16 June 2016

### Keywords:

Ediacaran carbonates

Sr-isotope blind dating

U–Pb SHRIMP zircon geochronology

Sierras Pampeanas

SW Gondwana

## ABSTRACT

The Sierras de Córdoba Metasedimentary Series consists of marbles and metasiliciclastic rocks of Ediacaran to early Cambrian age (ca. 630 and 540 Ma) that underwent high-grade metamorphism during the collisional Pampean orogeny in the early Cambrian. The ages of the marbles were determined from the Sr-isotope composition (blind dating) of screened samples of almost pure calcite marble and were further constrained with C- and O-isotope data and U–Pb SHRIMP detrital zircon ages of an interbedded paragneiss. Two groups of samples are recognised with Sr-isotope composition ca. 0.7075 and 0.7085 that are considered stratigraphically significant. The first is inferred early Ediacaran, the second late Ediacaran to early Cambrian. The Sierras de Córdoba Metasedimentary Series is correlated for the first time with marble-bearing metasedimentary series in several sierras to the west and north of Sierras de Córdoba (e.g., the Difunta Correa Sedimentary Sequence and the Ancaján Series), implying that all were probably parts of an originally extensive sedimentary cover. These series bear evidence of sedimentary sources in the Mesoproterozoic (and Paleoproterozoic) basement of the Western Sierras Pampeanas (part of the large MARA continental block) and farther west (Laurentia?). In terms of the age of limestones/marbles and detrital zircon patterns, the Sierras de Córdoba Metasedimentary Series differs strongly from the older section of late Ediacaran to early Cambrian Puncoviscana Formation of northwestern Argentina, which mostly outcrops in northern Sierra Chica and Sierra Norte, with sedimentary input from western Gondwana sources.

The Sierras de Córdoba Metasedimentary Series and the Puncoviscana Formation were probably juxtaposed during the Pampean orogeny along a complex suture zone that was further folded and/or imbricated at mid-crustal depths. The peak of metamorphism was attained at  $527 \pm 2$  Ma. According to the evidence found here most of the Sierras Pampeanas to the west of the Sierras de Córdoba were part of the lower colliding plate during the final amalgamation of SW Gondwana.

© 2016 Elsevier B.V. All rights reserved.

## 1. Introduction

The Sierras Pampeanas of western and northwestern Argentina extend over a large N–S elongated area some 700 km long and 450 km wide (Fig. 1). The basement in this area consists of Palaeozoic to Mesoproterozoic igneous and metamorphic rocks. Minor

outcrops of basement are also found in other structural units of the Andean foreland, e.g., the Precordillera and the Puna. Unfossiliferous metasedimentary rocks are abundant in the basement, most of them displaying low- to high-grade regional metamorphism of different ages (see Rapela et al., 1998a, 2001; Ramos et al., 2010 for a review). Siliciclastic rocks are widespread, but marbles and calc-silicate rocks can be locally abundant. The latter represent former deposits of marine carbonates and provide constraints for stratigraphy and paleogeography through the

\* Corresponding author.

E-mail address: [juan.murra@unc.edu.ar](mailto:juan.murra@unc.edu.ar) (J.A. Murra).

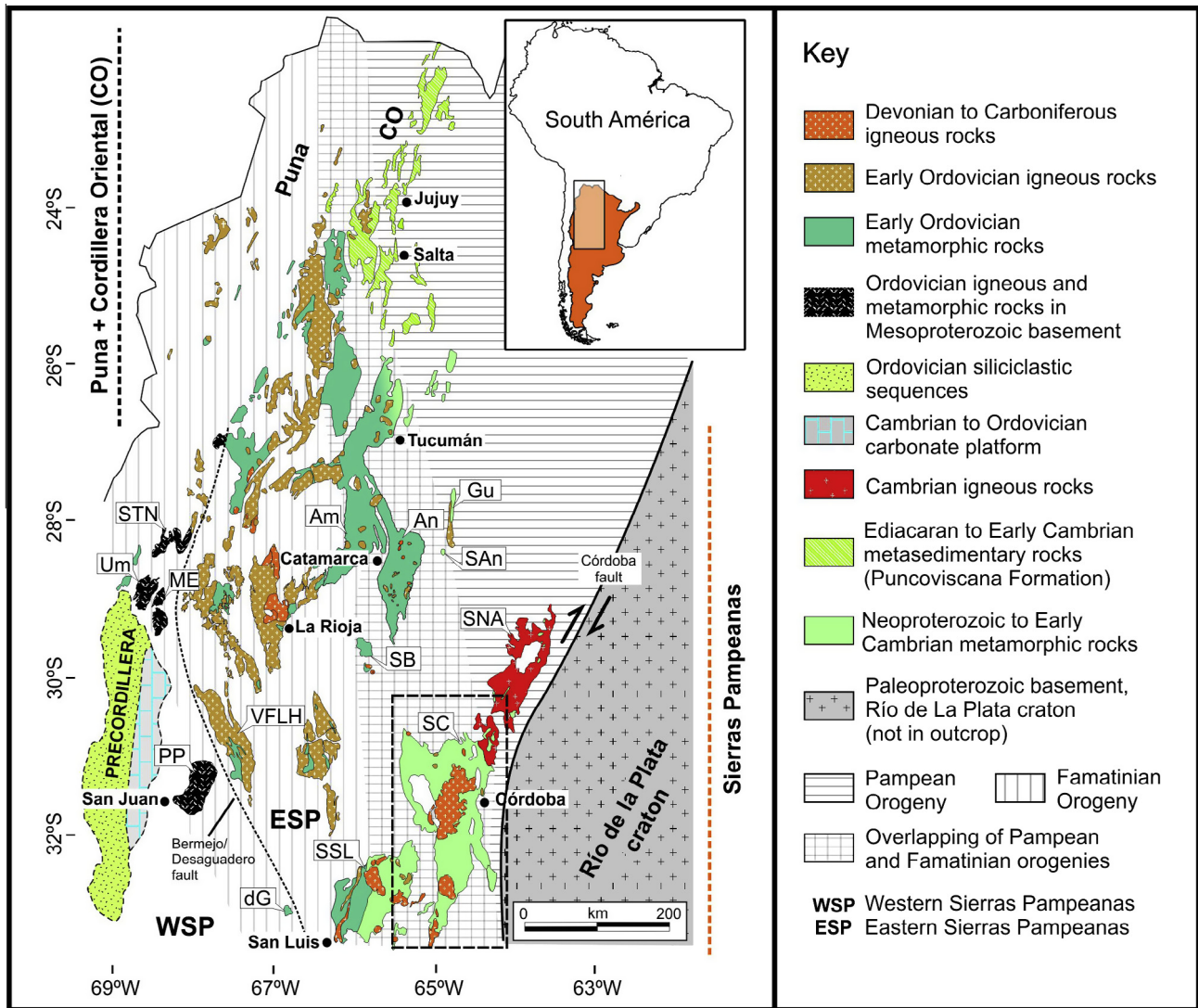


**Fig. 1.** Map of the Sierras Pampeanas (WSP and ESP) and northwestern Argentina. Main ranges abbreviations: Sierra de Ambato (Am), Sierra de Ancasti (An), Sierra de Guasayan (Gu), Sierra de Ancaján (SAN), Sierra del Toro Negro (STN), Sierra de Umango (Um), Sierras de Maz-Espinal (ME), Sierra Brava (SB), Sierra Norte-Ambargasta (SNA), Sierra de Valle Fertil-La Huerta (VFLH), Sierra de Pie de Palo (PP), Sierra del Gigante (dG), Sierra de Córdoba (SC) and Sierra de San Luis (SSL). Modified from Rapela et al. (2016).

application of isotope geochemistry methods (Sr, C and O) (Galindo et al., 2004; López de Azarevich, 2010; Murra et al., 2011 and references therein).

The Sr-isotope composition of marbles that remained unmodified after sedimentation has been increasingly used for chemical stratigraphy since the seminal work of Burke et al. (1982). These authors showed the  $^{87}\text{Sr}/^{86}\text{Sr}$  ratio in open-ocean limestone increased non-linearly over time because of a general predominance of input from continental radiogenic Sr compared to a juvenile contribution from the oceanic crust. Determination of this ratio has been particularly useful for dating Neoproterozoic and older carbonates where fossils are absent. Several compilations have been published showing the Sr-isotope composition of seawater vs. time for the Neoproterozoic era, some of them accompanied by  $\delta^{13}\text{C}$  values (and S and O-isotope systematics), to constrain the age of paleoclimatic changes (e.g., Derry et al., 1989, 1992; Jacobsen and Kaufman, 1999; Kuznetsov, 1998; Kuznetsov et al., 2013; Montañez et al., 2000; Halverson et al., 2007, 2010, among others).

We focus here on the Sr, C and O-isotope composition of marbles from the Sierras de Córdoba and easternmost Sierra de San

Luis (Eastern Sierras Pampeanas, ESP) (Figs. 1 and 2) and secondly on U–Pb SHRIMP zircon dating of interbedded metasiliciclastic rocks. It is the first time that this type of research has been carried out over such an extended region of the Sierras Pampeanas. Our results are significant for the provenance and timing of deposition, correlation with carbonate sequences elsewhere in the Sierras Pampeanas, and the tectonic evolution of the continental margin of SW Gondwana leading up to the Pampean orogeny.

## 2. Geological setting

The Sierras Pampeanas of Argentina can be divided into two groups separated by the Bermejo–Desaguadero first-order fault (Fig. 1):

- (1) the Western Sierras Pampeanas (WSP) consist of a Mesoproterozoic (and probably reworked Paleoproterozoic) basement of metabasites, orthogneisses, metasedimentary rocks (mainly gneisses and psammities with a few marbles), and massif-type anorthosites (Pankhurst and Rapela, 1998; Vujovich et al., 2004; Casquet et al., 2004, 2008; Rapela

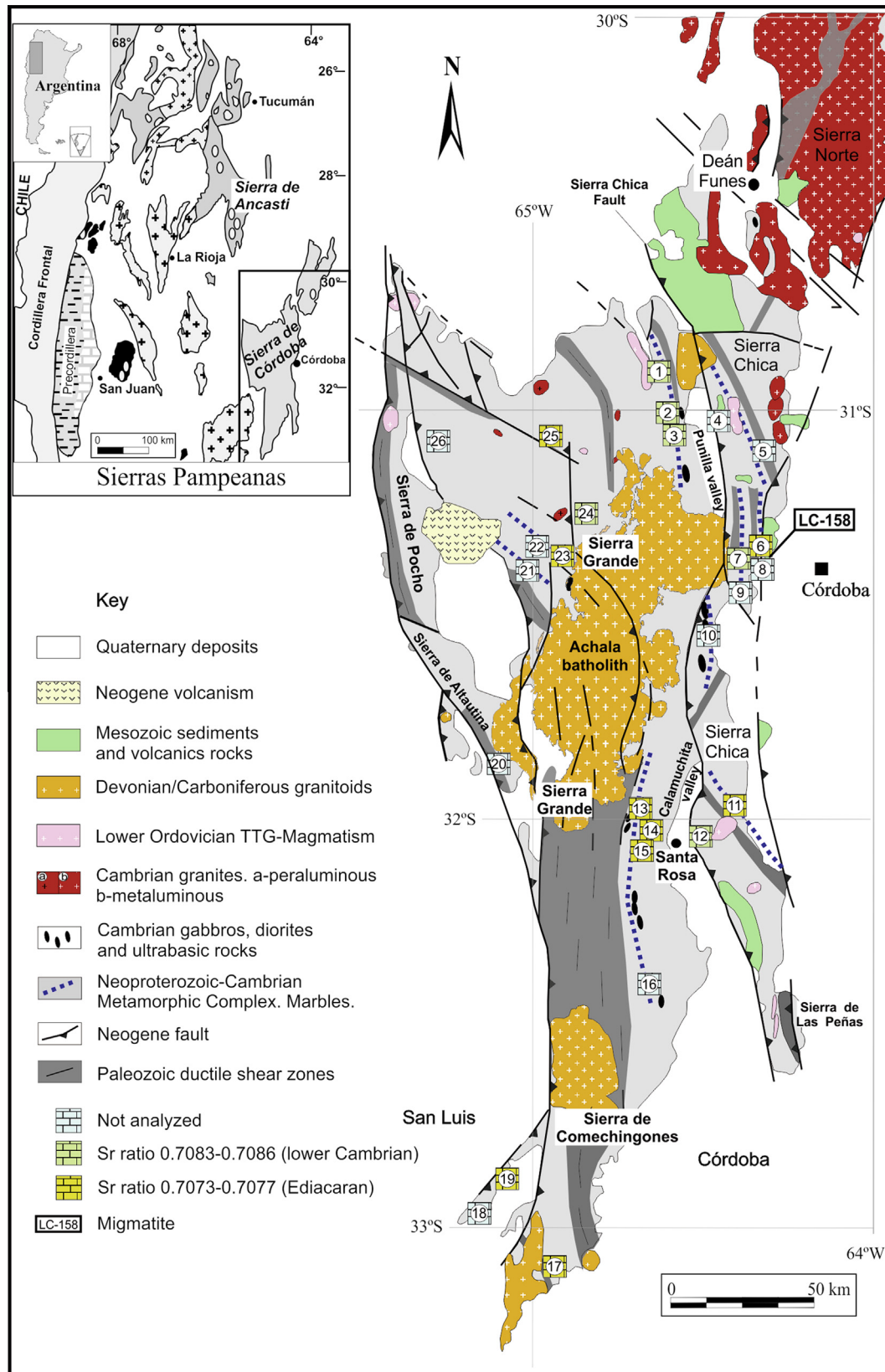


**Fig. 2.** Simplified geological map of the Sierras de Córdoba (after Martino, 2003 and Baldo et al., 2014) showing the main bands of marble and calcsilicate rocks. Sampling localities: 1-Quilpo; 2-Centenario; 3-La Falda; 4-El Cuadrado; 5-El Sauce; 6-Dumesnil; 7-Cantesur; 8-La Calera; 9-Las Jarillas; 10-Alta Gracia; 11-San Agustín; 12-Santa Rosa; 13-Sol de Mayo; 14-San Miguel; 15-Santa Mónica; 16-Cañada de Álvarez; 17-Achiras; 18-Lujan; 19-La Suiza; 20-Altautina; 21-Tala Cañada; 22-Cuchiyaco; 23-Igam; 24-Characato; 25-Iguazú; 26-Ciénaga del Coro.



et al., 2010) with a Neoproterozoic metasedimentary cover called the Difunta Correa Sedimentary Sequence including abundant marbles (Varela et al., 2001; Galindo et al., 2004). Both basement and cover experienced deformation and low- to high-grade metamorphism in the Famatinian orogeny (Early to middle Ordovician);

- (2) the Eastern Sierras Pampeanas consist of low to high-grade metasedimentary and plutonic rocks. The eastern part of the Eastern Sierras Pampeanas underwent Pampean orogeny (low- to high-grade metamorphism and magmatism) between 545 and 520 Ma (latest Ediacaran to early Cambrian), and was variably reworked by the Famatinian orogeny. The western part of the Eastern Sierras Pampeanas underwent the Famatinian orogeny only with abundant magmatism and low- to high-grade metamorphism from ~490 to 430 Ma (Sims et al., 1998; Pankhurst et al., 1998; Rapela et al., 1998a, 2007; Dahlquist et al., 2008).

The oldest sedimentary protoliths recorded so far in the easternmost part of the Eastern Sierras Pampeanas (phyllites to gneisses and metapsammities) have been correlated with the Puncoviscana Formation of northwestern Argentina (Cordillera Oriental). The Puncoviscana Formation basically is a sequence of pelitic-greywacke turbidites with locally interbedded conglomerates, limestones and volcanic rocks of late Neoproterozoic to Cambrian age (Omarini et al., 1999; Do Campo and Ribeiro Guevara, 2005; Toselli et al., 2005, 2010; Zimmermann, 2005; Adams et al., 2008; Escayola et al., 2011, among others). In the western Eastern Sierras Pampeanas two metasedimentary series are found: a late Neoproterozoic sequence with marbles (the Ancaján Series) in the sierras of Ancaján and Ancasti (Fig. 1) isotopically equivalent to the Difunta Correa Sedimentary Sequence of the Western Sierras Pampeanas (Murra et al., 2011; Rapela et al., 2016), and a sequence of typically banded schists (Ancasti Series) equivalent to the Puncoviscana Formation. Both series underwent low- to high-grade Famatinian metamorphism and deformation only, with no evidence so far of significant Pampean metamorphism. The contact between the two series is highly strained, suggesting tectonic juxtaposition.

### 3. Sierras de Córdoba Metasedimentary Series

The Sierras de Córdoba are the easternmost outcrops of the Eastern Sierras Pampeanas (Fig. 1). They consist of metasedimentary rocks, orthogneisses and plutonic rocks and dykes, locally covered by continental sediments of Carboniferous–Permian, Cretaceous and Cenozoic ages. The metasedimentary rocks are metapelites and metapsammities interbedded with widespread marbles and calc-silicate rocks (Gordillo, 1984; Gordillo and Bonalumi, 1987; Baldo, 1992; Guerreschi and Martino, 2002, 2003). Plutonism, deformation and metamorphism took place in the early Cambrian Pampean orogeny (Rapela et al., 1998b). Metamorphism reached medium to high temperature (600–800 °C) and intermediate pressure (4–8 kbar) (Gordillo and Lencinas, 1979; Rapela et al., 1998b, 2002; Steenken et al., 2010). Marbles are found as lenticular bodies due to stretching, but they can be followed over long distances with thicknesses from a few centimetres to hundreds of metres. They are often spatially associated with ductile shear zones and mafic to ultramafic igneous rocks (Martino, 2003). We will refer to this marble-bearing sequence as the “Sierras de Córdoba Metasedimentary Series”. Metasedimentary rocks equivalent to the Puncoviscana Formation of NW Argentina were recognised in the Sierras de Córdoba (Sierra Grande and in northwestern Sierra Chica and Sierra Norte) (Fig. 2) on the basis of detrital zircon ages (Escayola et al., 2007; Rapela et al., 2007, 2016). The term Puncoviscana Formation in the literature

embraces sedimentary rocks probably older, coeval and younger than the Pampean magmatic arc, with the only constraint that they are older than the unconformably overlying middle to late Cambrian Meson Group (e.g., Omarini et al., 1999; Adams et al., 2008, 2011; Escayola et al., 2011, and references therein). We restrict the term here to that part of the siliciclastic succession that is of relevance to the early history of the Puncoviscana sedimentary basin (e.g., Casquet et al., 2012). These rocks host the magmatic arc in the south (540–530 Ma) and can be coeval with syn-orogenic volcanism (ca. 530 Ma) in the north (Escayola et al., 2011).

The detrital zircon pattern of the Puncoviscana Formation in the Eastern Sierras Pampeanas is almost bimodal with characteristic peaks at ca. 1000 and 600 Ma. This pattern was interpreted as derived from West Gondwana sources in the east (Natal–Namaqua belt and probably the Brasiliano–Panafrican orogen and the huge East African orogen) (Schwartz and Gromet, 2004; Rapela et al., 2016). The maximum sedimentation age is 570 Ma and the uppermost part of the series contains interbedded tuffs of ca. 537 Ma (Escayola et al., 2011; von Gosen et al., 2014). Early Pampean orogeny magmatism in the Sierra Chica and Sierra Norte of Córdoba took place between 540 and 530 Ma (Rapela et al., 1998b; Schwartz et al., 2008; Iannizzotto et al., 2011). The relationship (age and structure) between the Puncoviscana Formation and the marble-bearing Sierras de Córdoba Metasedimentary Series has so far not been defined.

The  $^{87}\text{Sr}/^{86}\text{Sr}$  values and the C (and O-isotope in lesser degree) composition of limestones from the Puncoviscana Formation in NW Argentina suggest that they are early Cambrian (Sial et al., 2001; López de Azarevich, 2010; Toselli et al., 2012), consistent with the age of sedimentation between ca. 570 and 537 Ma yielded by the ages of detrital zircons in interbedded schists (Escayola et al., 2011; Casquet et al., 2012; Rapela et al., 2016). However, marbles of the Ancaján Series in the western Eastern Sierras Pampeanas (Sierra de Ancasti) yielded Sr-isotope ratios corresponding to the Ediacaran (Toselli et al., 2010; Murra et al., 2011), and the same Sr-isotope composition was found in marbles from the Difunta Correa Sedimentary Sequence in the Western Sierras Pampeanas (Sierras de Pie de Palo, Maz and Umango; Fig. 1) (Varela et al., 2001; Galindo et al., 2004). Recently Rapela et al. (2016) have confirmed that similarities between these two older series extend to the detrital zircon age patterns of siliciclastic rocks interbedded with the marbles and that these patterns differ from that of the Puncoviscana Formation. The Difunta Correa Sedimentary Sequence is thus apparently equivalent to the Ancaján Series, representing deposition across the tectonic boundary between the two groups of the Sierras Pampeanas (Fig. 1).

### 4. Sampling and analytical techniques

Sampling was designed to include most of the marble outcrops of the Sierras de Córdoba and easternmost Sierra de San Luis (Fig. 2). A total of 141 samples were collected, of which 49 were selected for petrography and chemistry. One sample was collected of migmatite interbedded with marble (Fig. 2) for U–Pb SHRIMP zircon geochronology to better constrain the age of the Sierras de Córdoba Metasedimentary Series and to strengthen correlations with sedimentary successions elsewhere in the Sierras Pampeanas.

To initially estimate the amount of calcite and dolomite, slabs (6 × 4 cm) were cut and the surface stained with alizarin (0.3 g of alizarin in 100 ml of 1.5% HCl solution) for 4 min and then gently washed in distilled water. The percentage of stained calcite in the slab surface was determined by computer imaging (using Image-J 1.48v, Rasband 1997–2015). Samples with calcite > 70% ( $n = 33$ ) were selected (Table 1). They were then analysed as in Murra et al. (2011) for Ca, Mg, Mn and Fe, and the insoluble residue (IR)

determined. Samples with low IR values were chemically screened according to the Mn/Sr, Mg/Ca and Fe/Sr ratios (Brand and Veizer, 1980; Melezhik et al., 2001 and references therein) to further select those that had not undergone significant post-sedimentary changes (Table 2): these were analysed for Sr, C and O-isotope composition.

Sr-isotope composition was determined at the Geochronology and Isotope Geochemistry Centre of the Complutense University, Madrid. To exclude contamination from other minerals, carbonate samples (~30 mg) were leached in a 10% acetic acid solution and then centrifuged to remove the insoluble residue (Fuenlabrada and Galindo, 2001). Additionally, the insoluble residue (IR as wt

%) was determined. The solution was subsequently evaporated and then dissolved in 3 ml of 2.5 N HCl. Sr was separated using cation-exchange columns filled with BioRad® 50 W X12 (200/400 mesh) resin. Procedural blank was less than 2 ng for Sr. The Sr-isotope composition was determined on an automated multicollector SECTOR 54® mass spectrometer and  $^{87}\text{Sr}/^{86}\text{Sr}$  values were normalised to a  $^{86}\text{Sr}/^{88}\text{Sr}$  value of 0.1194. The NBS-987 standard was routinely analysed along with our samples and gave an average  $^{87}\text{Sr}/^{86}\text{Sr}$  value of  $0.710251 \pm 0.00002$  ( $2\sigma$ ,  $n = 7$ ). Individual precision estimates (standard error on the mean) are given in Table 2; overall analytical uncertainty is estimated to be  $\pm 0.01\%$ . Most of the O and C-isotope determinations ( $n = 15$ ) were carried

**Table 1**  
Location, field description and petrography of marbles and migmatite LC-158.

Sample	Latitude	Longitude	Location		Rock description	% Calcite (staining)	Mineralogy (mineral abbreviation after Whitney and Evans, 2010)
CUA50*	31°07'37.2"	64°25'25.9"	Sierra Chica Belt	El Cuadrado	White, massive, middle-grained	54.67	Cal-Dol-Qz-Srp
ES01*	31°5'31.9"	64°19'21.3"		El Sauce	Green, banded, middle-grained	9.18	Dol-Cal-Srp-Phl-Di-Ep-Chl-Tr-Qz-Opq
Q01*	30°51'58.1"	64°41'06.5"		Quilpo	Bluish, massive, coarse-grained	69.87	Cal-Dol-Di-Wo-Qz-Phl-Opq
Q02	30°51'58.1"	64°41'06.5"			Pinkish, massive, coarse-grained	98.1	Cal-Qz-Phl-Ttn-Tr-Tlc
Q04b	30°51'58.1"	64°41'06.5"			White, massive, fine-grained	97.64	Cal-Qz-Tlc-Di
Q08	30°51'55.9"	64°41'32.7"			White, massive, coarse-grained	98.5	Cal-Qz-Phl-Di-Tlc-Opq
Q09	30°51'55.9"	64°41'32.7"			Pinkish, massive, coarse-grained	93.58	Cal-Qz-Ttn-Phl-Tcl
Q14	30°52'1.5"	64°40'58.6"			White, massive, coarse-grained	98.62	Cal-Qz-Ttn-Phl-Tlc
Q21	31°02'0.3"	64°33'39.6"		Centenario	Pinkish, massive, coarse-grained	92.1	Cal-Dol-Qz-Di-Phl-Opq-Ol-Srp
Q22*	31°02'0.3"	64°33'39.6"			White, massive, coarse-grained	67.75	Cal-Dol-Qz-Ttn-Phl
Q25b	31°5'53.1"	64°31'56.3"		La Falda	White, massive, coarse-grained	97.57	Cal-Qz-Phl-Ap-Opq-Ttn
Q27	31°5'53.1"	64°31'56.3"			Pinkish, massive, coarse-grained	97.84	Cal-Dol-Qz-Ttn-Di-Phl-Tlc
AG03*	31°38'20.9"	64°28'52.8"		Alta Gracia	White, banded, middle-grained	19.2	Cal-Dol-Ol-Di-Phl-Srp
AG04*	31°40'20.8"	64°26'37.8"			Grey, banded, middle to fine-grained	68.7	Cal-Dol-Ol-Phl-Di-Srp-Opq
CAN35	31°21'10.1"	64°20'58"		Cantesur	White to pinkish, fine-grained, mylonitized	96.68	Cal-Di-Ttn-Tr-Pl-Qz
D32	31°18'31.7"	64°20'05.2"		Dumesnil	White to pinkish, massive, middle-grained	99.5	Cal-Dol-Qz-Phl-Di
D33*	31°18'31.7"	64°20'05.2"			White, massive, fine-grained	45.3	Cal-Dol-Srp-Phl
D37	31°18'31.7"	64°20'05.2"			Pinkish, banded, coarse-grained	98.23	Cal-Grt-Qz-Phl-Opq-Di
D38*	31°18'31.7"	64°20'05.2"			Pinkish, massive, middle-grained	48.84	Cal-Dol-Srp-Ol-Di
D40	31°18'31.7"	64°20'05.2"			White, massive, coarse-grained	97.83	Cal-Qz-Opq-Tr-Phl-Mc-Di
D41*	31°18'31.7"	64°20'05.2"			White, massive, middle-grained	77.95	Cal-Dol-Srp-Ol-Phl
LC-158*	31°21'37.6"	64°20'59.7"		La Calera	Granoblastic/lepidoblastic lenses – fine to middle-grained	No data	Qz-Grt-Pl-Bt- ± Sil-[Zrn-Ep-Opq-Ap]
LJ143*	31°35'29.6"	64°34'59.4"		Las Jarillas	White, massive, coarse-grained	12.17	Dol-Tr-Phl-Chl-Cal
CA69*	32°24'37.4"	64°31'55.6"		Cañada de	White, massive, coarse-grained	15.68	Dol-Phl-Ser-Tr- ± Cal
CA71a*	32°24'10.1"	64°31'44.8"		Álvarez	Bluish, massive, coarse-grained	9.21	Dol-Srp-Di-Phl-Ol- ± Cal
SA1*	32°00'10.5"	64°24'29.1"		San Agustín	White, banded, coarse-grained	0.5	Dol-Phl-Srp-Tlc-Chl
SA56	31°56'12.9"	64°25'9.9"			White, massive, fine-grained	98.54	Cal-Qz-Tr-Opq
SM81*	32°03'30"	64°41'45.4"		Sta. Mónica	White, massive, coarse-grained	84.02	Cal-Dol-Iddingsite
SM82	32°03'30"	64°41'45.4"			Pinkish, banded, coarse-grained	95.06	Cal-Qz-Ttn-Phl
SMi87	32°02'48.4"	64°43'57"		San Miguel	Pinkish, banded, fine-grained	96	Cal-Qz-Pl-Ttn-Di-Tr-Phl
SOL91*	31°59'25.8"	64°43'32.6"		Sol de	White, banded, fine-grained	83.78	Cal-Dol-Pl-Srp-Qz
SOL92	31°59'25.8"	64°43'32.6"		Mayo	White, banded, coarse-grained	92.02	Cal-Phl-Qz-Tr-Di-Dol
SR77*	32°04'50"	64°27'59.8"		Sta. Rosa	White, massive, fine-grained	69.33	Cal-Phl-Qz-Anf-Iddingsita
SR79	32°04'50"	64°27'59.8"			White, massive, coarse-grained	95	Cal-Qz-Di-Ttn-Gr
AL135*	31°45'53.7"	65°09'21.4"		Altautina	White, massive, coarse-grained	8.85	Dol-Phl-Di-Tr ± Cal
BN	31°7'57.2"	64°46'48.3"		Characato	Bluish, massive, coarse-grained	79.35	Cal-Qtz-Tr-Di-Opq-Ttn ± Dol
CU126*	31°19'48.2"	65°01'54.9"		Cuchiyaco	White, banded, middle-grained	18.79	Dol-Cal-Tlc-Phl-Di-Srp-Ol-Spl-Opq
IG101	31°15'3.20"	64°49'11.1"		Igam	White, massive, coarse-grained	74.6	Cal-Qz-Di- ± Dol
IG102	31°15'3.20"	64°49'11.1"			Grey, massive, coarse-grained	73.46	Cal-Tr-Qz-Opq- ± Dol
IG104	31°15'3.20"	64°49'11.1"			Grey, banded, middle to fine-grained	81.98	Cal-Qtz-Tr-Di-Opq-Ttn ± Dol
IGU178	31°03'49"	64°47'34.1"		Iguazú	Grey, massive, coarse-grained	93.16	Cal-Qz-Opq
IGU179	31°03'49"	64°47'34.1"			Grey, banded, middle-grained	76.61	Cal-Qz-Opq-Tr ± Dol
IGU180*	31°01'03.7"	64°50'32.6"			Grey, banded, middle to fine-grained	97.35	Cal-Qz-Opq-Tr-Phl
SG172	31°05'35.4"	64°48'27.2"		San Gregorio	White, massive, coarse-grained	97.48	Cal-Phl-Qz
TC121*	31°22'44.2"	65°03'11.5"		Tala Cañada	White, massive, fine-grained	26.9	Dol-Di-Opq-Qz-Cal
LC193*	32°56'34.8"	65°08'18.7"	Other locations	San Luis	Grey, massive, fine-grained	74.12	Cal-Tr-Qz-Gr ± Dol
LC194	32°56'34.8"	65°08'18.7"			Grey, banded, middle to fine-grained	93.04	Cal-Tr-Qz-Gr
LC195	32°56'34.8"	65°08'18.7"			Grey, massive, coarse-grained	85.28	Cal-Tr-Qz-Gr ± Dol
AC60	33°08'43.1"	64°57'15.9"		Achiras	White, massive, fine-grained	75.5	Cal-Dol-Qz-Tr-Phl-Di-Phl
AC61a	33°08'43.1"	64°57'15.9"			Grey, banded, middle to fine-grained	97.36	Cal-Dol-Tr-Phl-Qz

\* Not analysed for geochemistry.

**Table 2**

Elemental and isotopic composition of Sr, C and O marbles. [IR %]: insoluble residue.

Sample	Location	Rb (ppm)	Sr (ppm)	<sup>87</sup> Sr/ <sup>86</sup> Sr	δ <sup>13</sup> C <sub>PDB</sub> ‰	δ <sup>18</sup> O <sub>PDB</sub> ‰	Ca % weight	Mg % weight	Fe (ppm)	Mn (ppm)	Mg/Ca	Mn/Sr	IR %
Q02	Sierra Chica Belt	<0.2	499	0.70834			42.33	0.057	489	0.39	0.0013	0.0008	2
Q04b			767	0.70835	1.89	−6.54	44.15	0.009	297	0.79	0.0002	0.001	0.14
Q08			505	0.70835			42.42	0.1	528	0.4	0.0024	0.0008	0.26
Q09			612	0.70837	1.63	−10.84	45.05	0.03	1105	1.24	0.0007	0.002	1.88
Q14	Centenario	<0.2	581	0.70834			51.41	0.021	579	22.12	0.0004	0.0381	2.65
Q21			344	0.70848			46.12	0.032	1149	24.29	0.0007	0.0706	2.53
Q25b			463	0.70834	2.03	−6.14	43.28	0.029	441	0.58	0.0007	0.0012	0.96
Q27			1162	0.70836	1.74	−8.05	31.39	0.292	2080	70.86	0.0093	0.0609	4.47
CAN35	Cantesur		398	0.70850	0.81	−9.14	41.26	0.031	852	0.32	0.0007	0.0008	2.14
D32			1214	0.70765	−1.05	−8.06	42.86	0.049	1319	62.7	0.0011	0.0516	0.18
D37			1038	0.70771	−0.91	−7.8	45.53	0.035	2351	74.29	0.0008	0.0715	0.57
D40			876	0.70765	−0.59	−6.03	43.82	0.016	2161	25.28	0.0004	0.0288	0.4
SA56	San Agustín		324	0.70769	−0.16	−8.88	39.88	0.03	1742	48.93	0.0007	0.1512	1.2
SM82			816	0.70747	1.96	−9.32	44.58	0.036	2187	87.67	0.0008	0.1074	2.49
SMi87			1828	0.70752	3.25	−12.05	30.45	0.768	1366	255.29	0.0252	0.1396	3.87
SOL92			797	0.70751	3.54	−10.4	37.74	0.133	896	57.02	0.0035	0.0715	1.63
SR79	Sierra Grande Belt	<0.2	1137	0.70860	1.07	−8.74	38.04	0.002	873	30.1	0.0001	0.0265	1.54
BN			2497	0.70836	0.73	−5.25	34.36	0.01	11	0.42	0.0003	0.0002	1.5
IG101			2456	0.70737			31.92	0.141	59	4.84	0.0044	0.0019	2.7
IG102			3513	0.70736	2.98	−5.14	32.51	0.117	47	1.32	0.0036	0.0004	3.09
IG104	San Gregorio	<0.2	3120	0.70737	3.09	−4.86	33.50	0.097	51	8.71	0.0029	0.0028	2.1
SG172			1304	0.70848			40.77	0.11	n.d	0.59	0.0027	0.0004	1.94
IGU178			828	0.70737	3.2	−9.14	32.84	0.507	n.d	0.86	0.0015	0.0010	1.48
IGU179			3012	0.70740			33.35	0.456	n.d	0.35	0.0013	0.0001	7.58
AC60	Other locations		1981	0.70764	2.78	−7.91	27.95	0.771	343	126.28	0.0276	0.0637	4.03
AC61a			613	0.70743			35.28	0.083	305	0.83	0.0023	0.0013	1.25
LC194			305	0.70764			33.85	0.438	n.d	0.2	0.0129	0.0006	5.48
LC195			2106	0.70786			35.52	0.611	n.d	0.22	0.0172	0.0001	6.03

n.d. = No detected.

out on a double inlet Micromass SIRA-II® mass spectrometer at the Isotope Laboratory of Salamanca University (ILSU) following the method of McCrea (1950). Three samples (Q-09, IG-102 and IGU-178) were analysed using direct injection into a GasBench/MAT-23 Mass spectrometer at the CAB (Centro de Astrobiología, CSIC). Rocks were first reacted with 100% orthophosphoric acid at 25 °C to liberate CO<sub>2</sub>. O-isotope compositions were corrected following Craig (1957). O and C-isotope compositions are reported in δ (‰) notation on the PDB scale. Analytical errors (1σ) are ±0.057‰ for C and ±0.198‰ for O (ILSU) and 0.035‰ for C and 0.1‰ for O (CAB). Results are shown in Table 2.

Rb was determined in four samples with different Sr contents and Sr-isotope compositions to check for the effect of <sup>87</sup>Rb decay on the initial Sr-isotope composition. The samples were reacted with 0.5 M acetic acid, centrifuged at 4000 rpm and the leachate collected for analysis. The residue was washed twice with millipore water centrifuged and the new leachate added to the first. The leachates were dried and re-dissolved with 1 ml of 0.1 M HNO<sub>3</sub> for analysis by ICP-MS. All four samples yielded Rb contents below detection limit, i.e., <0.2 ppm.

Sample LC-158 was analysed at the Centro de Instrumentación Científica de Granada (Spain) using SHRIMP Ile/mc, following the method described by Montero et al. (2014). Results are shown in Fig. 9 as Tera-Wasserburg and density probability plots produced using ISOPLOT/Ex (Ludwig, 2003). For ages less than 1.1 Ga the <sup>207</sup>Pb-corrected <sup>206</sup>Pb/<sup>238</sup>U age (Williams, 1998) was preferred; otherwise choice between the <sup>204</sup>Pb-corrected <sup>206</sup>Pb/<sup>238</sup>U and <sup>207</sup>Pb/<sup>206</sup>Pb age was based on the relative age uncertainty, discounting any that were >10% discordant (Table 3).

## 5. Marble outcrops and petrography

The main marble outcrops are concentrated in the central-eastern Sierras de Córdoba defining two main belts: the Sierra Chica belt on the east and the Sierra Grande belt on the west. The two belts are separated by the Valle de Punilla – Calamuchita Cenozoic thrust system. The Sierra Chica belt shows the more abundant marble outcrops. The Sierra Grande belt runs to the north and west of the large Devonian Achala batholith (Fig. 2) (Lira and Sfragulla, 2014 and references therein). Small marble outcrops are also found in the southern part of Sierra Grande and the easternmost Sierra de San Luis (Costa et al., 2001) (Fig. 2). The outcrops are tectonically repeated by folding and/or thrusting, and often isolated because of stretching (boudinage): their original disposition remains unknown.

Most samples were collected in quarries, either inactive or still exploited for various uses such as the cement industry (e.g., Fig. 3). In all cases the host rocks are migmatites, gneisses, schists and calc-silicate rocks (Bonalmi et al., 1999). Marbles are white to pink and medium to coarse-grained. A decimetre-scale banding between almost pure and impure marble is common (Table 1, Figs. 3 and 4). Mineral composition can be summarised as: Cal (73–98% modal) ± Dol – Qz – Di – Tr – Phl – Ttn – Gr – Tlc – Wo – Opq (mineral abbreviations after Whitney and Evans, 2010). Texture is granoblastic with calcite grains 0.5 mm in size on average, evolving into porphyroclastic with grain-size reduction near the shear zones. In some outcrops in central Sierra Chica ca. 1 m thick dykes of fine-grained tonalite of unknown age intruded the marbles. Other rocks found within the marble outcrops are disrupted

**Table 3**  
Summary of SHRIMP U–Pb zircon results for sample LC-158.

Grain spot	U ppm	Th ppm	Th/U	<sup>206</sup> Pb ppm	ε <sub>506</sub> ‰	Total ratios			Radiogenic ratios			Ages			Preferred age (Ma)		
						<sup>207</sup> Pb/ <sup>238</sup> U	±	<sup>206</sup> Pb/ <sup>238</sup> U	±	<sup>206</sup> Pb/ <sup>238</sup> U	±	<sup>207</sup> Pb/ <sup>235</sup> U	±	<sup>207</sup> Pb/ <sup>206</sup> Pb	±	% Disc	±
1	155.7	114.4	0.75	42.0	-0.15	0.12180	0.00214	0.31175	0.00527	0.00246	0.03124	0.00529	5.28827	0.13994	0.461	1751.2	260
2	173.7	46.7	0.28	23.0	0.13	0.06962	0.00164	0.15303	0.00438	0.00487	0.04170	0.00139	0.00139	0.13994	0.461	917.9	273
3	67.8	55.7	0.84	21.9	0.23	0.12893	0.00082	0.37410	0.00356	0.00911	0.12045	0.00355	6.55029	0.07883	0.569	2045.3	11.4
5	111.7	57.1	0.52	32.1	-0.19	0.11906	0.00164	0.33166	0.00911	0.00166	0.33219	0.00912	5.16174	0.07066	0.639	1849.0	24.4
6	76.1	31.0	0.42	13.0	0.00	0.07976	0.00014	0.19699	0.00477	0.00797	0.07976	0.00477	2.16628	0.05315	0.710	1159.1	3.4
7	538.6	435.5	0.83	155.2	-0.01	0.12205	0.00611	0.33300	0.02941	0.00611	0.12212	0.00611	5.60771	0.05694	0.626	1853.0	86.4
8	191.1	95.1	0.51	33.5	0.02	0.07991	0.00089	0.20234	0.00218	0.00797	0.07977	0.00218	2.22507	0.03574	0.484	1187.7	11.7
9	266.3	154.8	0.60	46.9	0.13	0.08109	0.00072	0.20367	0.00343	0.00804	0.08004	0.00343	2.24483	0.04362	0.623	1193.6	17.8
10	86.5	38.2	0.45	11.3	-0.09	0.06829	0.00072	0.15062	0.00407	0.00436	0.04345	0.00210	0.00210	0.04362	0.623	905.4	24.5
11	177.8	89.7	0.52	36.2	-0.09	0.08481	0.00310	0.23466	0.01880	0.00853	0.03010	0.00882	2.77331	0.24384	0.655	1361.5	99.0
12	136.8	187.4	1.41	32.8	0.13	0.11635	0.00121	0.27684	0.00719	0.01535	0.00125	0.00718	4.39786	0.12480	0.659	1573.8	19.4
13	73.3	26.9	0.38	12.7	0.16	0.07973	0.00067	0.19995	0.00599	0.00750	0.00888	0.00598	2.16100	0.06951	0.671	1173.5	32.2
14	93.0	39.7	0.44	16.1	0.00	0.07801	0.00075	0.20047	0.00572	0.00780	0.00780	0.00572	2.15630	0.06540	0.678	1177.8	30.8
15	125.6	26.5	0.22	27.6	0.07	0.09742	0.00242	0.25371	0.01498	0.00968	0.02462	0.01497	3.38805	0.21802	0.660	1456.7	77.4
16	168.6	78.3	0.48	35.2	0.00	0.08302	0.00123	0.24086	0.01231	0.00830	0.00131	0.01477	2.75634	0.14775	0.686	1391.1	64.2
17	147.4	128.5	0.89	42.9	-0.01	0.12386	0.00240	0.33618	0.01625	0.01297	0.00241	0.01625	5.74715	0.30003	0.667	1868.5	78.9
18	238.3	181.1	0.78	38.7	-0.01	0.07543	0.00062	0.18759	0.00296	0.00751	0.00662	0.00296	1.95326	0.03542	0.627	1108.4	16.1
19	97.0	182.9	1.93	13.3	0.47	0.07212	0.00097	0.15831	0.00517	0.01799	0.00557	0.00174	0.00174	0.03542	0.627	945.6	31.1
20	164.2	69.5	0.43	26.7	-0.07	0.07790	0.00090	0.18813	0.00401	0.00784	0.00092	0.00401	2.03613	0.04998	0.625	1111.9	21.8
21	195.3	146.9	0.77	49.9	0.07	0.10273	0.00098	0.29533	0.00716	0.01021	0.00951	0.00716	4.15943	0.10994	0.661	1667.2	35.7
22	195.3	100.3	0.53	41.0	0.06	0.08586	0.00114	0.24287	0.00703	0.00836	0.00114	0.00703	2.85675	0.09171	0.649	1400.9	36.6
23	253.1	13.9	0.06	18.2	0.27	0.05708	0.00147	0.08293	0.00132	0.00829	0.00132	0.00472	0.00472	0.09171	0.649	513.9	9.0
24	107.5	32.3	0.31	18.8	0.52	0.07871	0.00152	0.20235	0.01002	0.00745	0.00207	0.00998	2.07277	0.11785	0.627	1182.8	53.8
25	47.4	53.6	1.16	9.1	0.15	0.08988	0.00220	0.22174	0.01102	0.00871	0.00291	0.01101	2.70839	0.16159	0.600	1289.4	58.3
26	291.9	9.7	0.03	21.9	0.14	0.05923	0.00056	0.08653	0.00105	0.00840	0.00114	0.00243	0.00243	0.16159	0.600	534.2	6.7
27	74.8	35.8	0.49	10.7	0.00	0.07147	0.00066	0.16536	0.00418	0.01647	0.00450	0.00146	0.00146	0.16159	0.600	987.1	24.9
28	119.1	126.3	1.09	19.1	0.30	0.07687	0.00082	0.18543	0.00162	0.00748	0.00088	0.00161	1.89888	0.02865	0.416	1095.3	10.3
29	157.1	53.5	0.35	24.0	0.04	0.07382	0.00086	0.17622	0.00444	0.00747	0.00107	0.00444	1.78436	0.05237	0.618	1046.7	26.7
30	98.9	35.6	0.37	20.9	-0.16	0.09028	0.00100	0.24371	0.00759	0.00914	0.00168	0.00761	3.08068	0.11194	0.618	1407.8	39.5
31	325.6	84.4	0.27	57.4	0.03	0.07966	0.00044	0.20352	0.00289	0.00794	0.00046	0.00289	2.22836	0.03516	0.648	1193.9	15.5
32	343.9	16.6	0.05	25.7	0.39	0.05838	0.00064	0.08648	0.00130	0.00845	0.00140	0.00393	0.00393	0.03516	0.648	534.5	8.3
33	115.1	57.9	0.52	18.5	0.09	0.07773	0.00048	0.18546	0.00306	0.00702	0.00057	0.00306	1.96787	0.03634	0.644	1094.3	18.2
34	331.0	11.6	0.04	24.7	0.09	0.05725	0.00083	0.08610	0.00077	0.00618	0.00087	0.00270	0.00270	0.03634	0.644	532.9	5.2
35	204.1	9.8	0.05	15.2	0.00	0.05670	0.00031	0.08608	0.00127	0.00623	0.00134	0.00331	0.00331	0.03634	0.644	533.2	8.0
36	302.4	9.7	0.03	22.2	0.21	0.05753	0.00020	0.08494	0.00033	0.00496	0.00036	0.00270	0.00270	0.03634	0.644	525.7	2.2
37	264.8	12.8	0.05	19.5	-0.01	0.05837	0.00079	0.08489	0.00131	0.00481	0.00141	0.00492	0.00492	0.03634	0.644	524.8	8.4
38	112.5	46.6	0.42	19.9	0.14	0.07995	0.00173	0.20434	0.00458	0.00785	0.00177	0.00458	2.21876	0.07094	0.505	1197.2	24.6
39	557.4	27.3	0.05	70.5	0.05	0.08188	0.00080	0.14618	0.00181	0.00152	0.00082	0.00181	1.64240	0.02686	0.546	864.4	12.2
40	356.8	98.4	0.28	60.2	0.25	0.08118	0.00288	0.19504	0.00570	0.07920	0.00297	0.00569	2.12494	0.11194	0.441	1146.2	30.8
41	517.3	18.7	0.04	38.3	0.00	0.05833	0.00079	0.08543	0.00426	0.00539	0.00442	0.00292	0.00292	0.11194	0.441	528.2	26.3
42	272.7	12.2	0.05	20.2	0.07	0.05935	0.00018	0.08562	0.00052	0.00545	0.00053	0.00204	0.00204	0.11194	0.441	528.6	3.2
43	349.1	12.1	0.04	25.6	0.12	0.05814	0.00046	0.08483	0.00053	0.00480	0.00060	0.00254	0.00254	0.11194	0.441	524.7	3.6
44	278.0	11.0	0.04	20.4	0.00	0.05657	0.00048	0.08537	0.00054	0.00552	0.00162	0.00256	0.00256	0.11194	0.441	529.0	9.6
45	153.4	58.3	0.39	33.6	0.07	0.09310	0.00099	0.25299	0.00335	0.00925	0.00100	0.00335	3.22614	0.05643	0.545	1453.0	17.2
46	389.4	11.1	0.03	28.6	0.08	0.05812	0.00083	0.08486	0.00269	0.00483	0.00283	0.00256	0.00256	0.05643	0.545	524.9	16.8
47	153.2	65.9	0.44	27.9	0.07	0.08008	0.00089	0.21043	0.00637	0.07955	0.00093	0.00637	2.30669	0.07532	0.668	1230.4	34.0
48	261.0	170.4	0.67	11.1	0.05	0.05277	0.00107	0.04895	0.00077	0.04894	0.00086	0.00152	0.00152	0.07532	0.668	308.0	5.3
49	458.2	10.5	0.02	33.6	0.19	0.05924	0.00020	0.08480	0.00143	0.00463	0.00146	0.00302	0.00302	0.07532	0.668	523.7	8.7
50	275.3	38.4	0.14	39.9	-0.05	0.07525	0.00050	0.16751	0.00229	0.16686	0.00249	0.00796	0.00796	0.07532	0.668	994.8	13.8
51	196.8	108.1	0.56	19.8	-0.15	0.06381	0.00059	0.11653	0.00181	0.01641	0.00195	0.00399	0.00399	0.07532	0.668	709.9	11.3
52	129.9	34.7	0.27	22.0	0.12	0.08186	0.00039	0.19562	0.00337	0.08095	0.00150	0.01954	0.01954	0.07532	0.668	1150.6	18.2
53	217.1	62.6	0.30	39.4	0.07	0.08102	0.00068	0.20961	0.00212	0.08047	0.00070	0.00212	2.32411	0.03205	0.528	1226.0	11.3
54	264.8	11.8	0.05	19.5	0.20	0.05905	0.00074	0.08520	0.00048	0.00506	0.00056	0.00301	0.00301	0.03205	0.528	526.3	3.3
55	171.9	70.7	0.42	29.5	-0.08	0.08006	0.00191	0.19825	0.00393	0.08064	0.00193	0.01939	2.20588	0.06914	0.456	1166.6	21.2
56	262.7	66.5	0.26	45.6	0.08	0.08058	0.00024	0.20049	0.00348	0.07995	0.00042	0.00348	2.20854	0.04081	0.676	1177.2	18.7

Notes: 1. Uncertainties given at the two σ level.

2. For areas younger than 1100 Ma correction for common Pb made using the measured <sup>238</sup>U/<sup>206</sup>Pb and <sup>207</sup>Pb/<sup>206</sup>Pb ratios.

3. For areas older than 1100 Ma correction for common Pb made using the measured <sup>204</sup>Pb/<sup>206</sup>Pb.



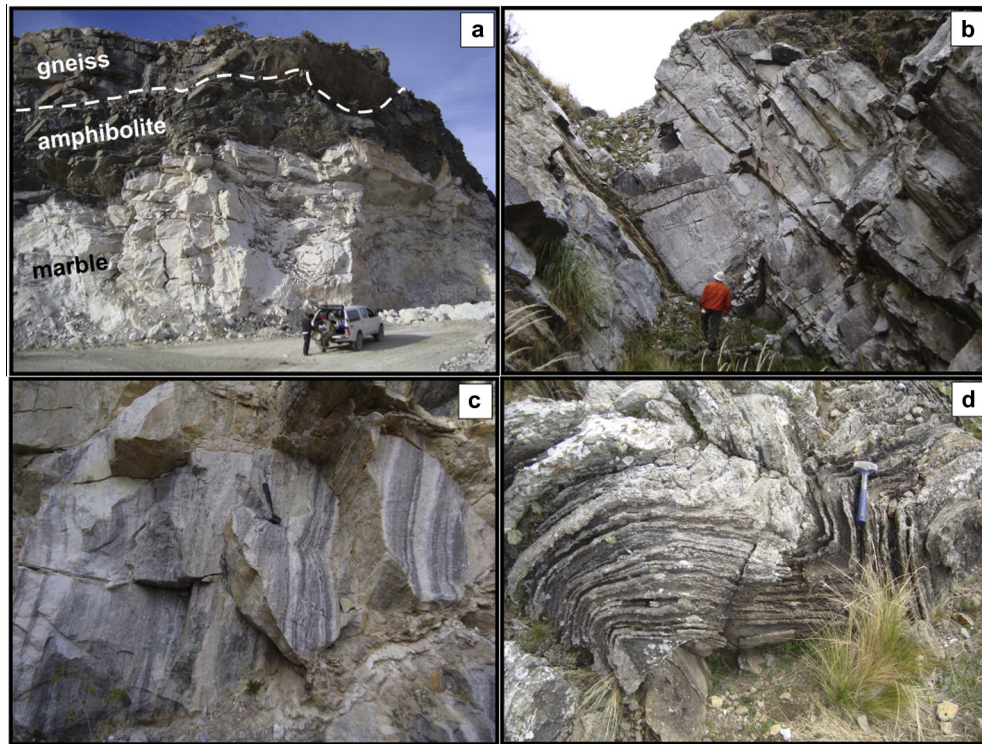


**Fig. 3.** (a) Pure white marble in contact with amphibolites in the Quilpo quarry, Sierra Chica belt; (b) marble with interbedded metapelites near the IGAM quarry, Sierra Grande belt; (c) banded marble in the La Suiza quarry, San Luis; (d) folded marble in the Dumesnil quarry, Sierra Chica belt.

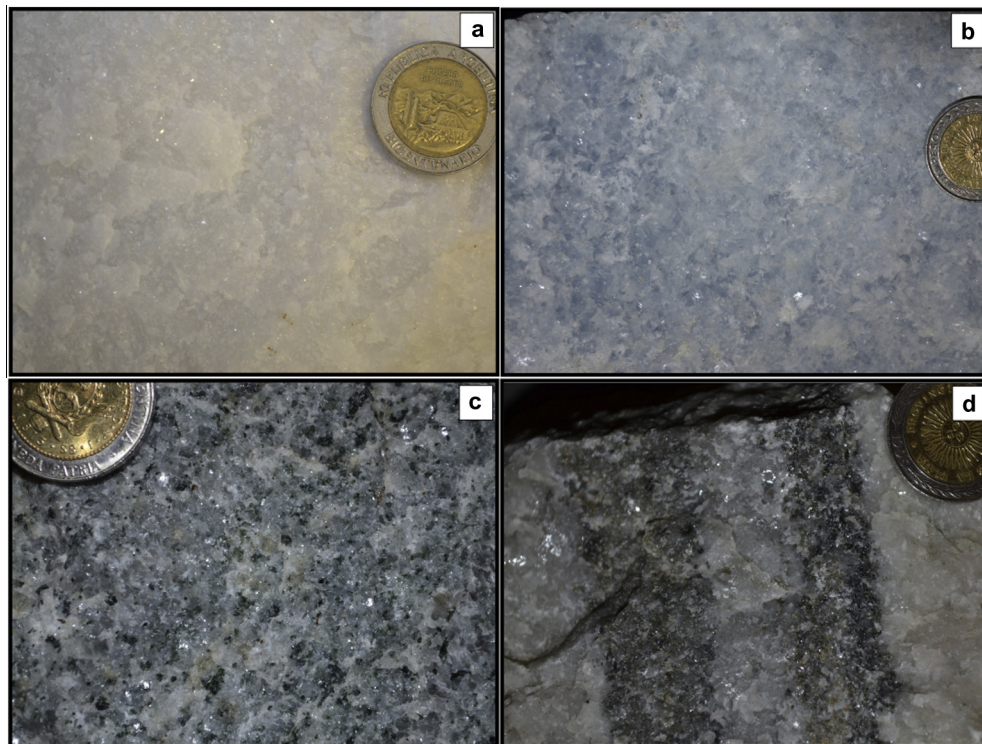


**Fig. 4.** Close-up view of marble types: (a) pure white fine-grained (Quilpo quarry, Sierra Chica belt); (b) pure bluish coarse-grained (Characato, Sierra Grande belt); (c) grey massive coarse-grained (Iguazú quarry, Sierra Grande belt); (d) grey to white banded medium to coarse-grained (La Suiza quarry, San Luis).

amphibolite lenses 5–20 m long and sporadic layers of impure metapsammite and/or quartzite.

The migmatite sample (LC-158) for U–Pb SHRIMP zircon geochronology was collected from a succession of gneisses and

migmatites interbedded with amphibolites and marbles at La Calera near Córdoba (Baldo et al., 1996) (Table 1, Figs. 2 and 5). It is a metatexite consisting of Qz – Grt – Pl – Bt –  $\pm$ Sil, with Zrn – Ep – Opq – Ap accessories. Foliation is defined by granoblastic



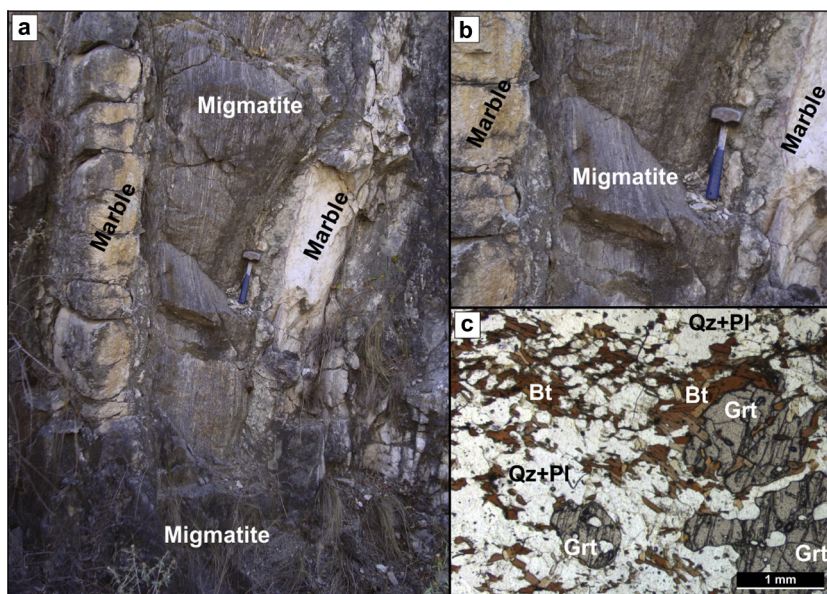


**Fig. 5.** (a) Migmatite (stromatolite) interbedded with marbles, where sample LC-158 was collected; (b) outcrop view; (c) photomicrograph of LC-158 (plane polarized light) showing irregular garnet grains.

Qz + Pl lenses alternating with biotite-rich bands that wrap around garnet porphyroclasts up to 2 mm in size. The latter contain inclusions of biotite, quartz and sillimanite.

## 6. Isotope composition

### 6.1. The Sierra Chica belt

Seventeen samples were analysed from this belt. They are calcite marbles with contents of Ca = 30.45–51.41 wt%; Mg = 0.002–0.768 wt%; Sr = 324–1828 ppm, Fe = 297–2351 ppm and Mn between <1 and 255 ppm (Table 2). The content of non-carbonate minerals (as insoluble residue, IR) is low, between 0.14 and 4.47 wt% (Table 2). The higher IR values (e.g., in samples Q-27 and SMi-87) correlate with decreased Ca and increased Mg and Mn; Fe contents are also relatively high. This evidence suggests that at least part of the Mg, Mn and Fe is contributed by the non-carbonate fraction of the marble. Most samples show Mn/Sr, Mg/Ca and Fe/Sr ratios compatible with little post-sedimentary alteration (Table 2 and Fig. 6). Only three samples show one or two elemental ratios higher than the boundary values for absence of alteration (Q-21, SA-26, SMi-87). The  $^{87}\text{Sr}/^{86}\text{Sr}$  ratios of the seventeen samples fall into two groups: ten samples between 0.70834 and 0.70860 and seven samples between 0.70747 and 0.70771, well outside error limits and the difference is therefore considered geologically significant (Table 2, Fig. 6). Measured Rb contents of four samples of the first group are negligible (<0.2 ppm) and cannot have contributed to the higher  $^{87}\text{Sr}/^{86}\text{Sr}$  ratios. Moreover, one of the three samples with relatively high elemental ratios referred to above is in the low  $^{87}\text{Sr}/^{86}\text{Sr}$  group, suggesting that small amounts of alteration have had minimal effect on Sr-isotope composition. C and O-isotopes were determined in twelve samples. The  $\delta^{13}\text{C}_{\text{PDB}}$  value ranges from  $-0.16$  to  $+3.54\text{‰}$ , compatible with a marine origin. All the samples with the more radiogenic Sr show positive values of  $\delta^{13}\text{C}_{\text{PDB}}$ , whereas the less radiogenic group shows both positive and negative values. The  $\delta^{18}\text{O}_{\text{PDB}}$  values range from  $-6.03$  to  $-12.05\text{‰}$  (most values  $> -10\text{‰}$ ), again suggesting little modification of the original marine composition (Table 2). The  $\delta^{18}\text{O}$  values of late Neoproterozoic carbonates are  $< -5\text{‰}$  (e.g., Jacobsen and

Kaufman, 1999). Values larger than  $-10\text{‰}$  are considered indicative of little post-sedimentary alteration (Letnikova et al., 2011). The lowest value ( $-12.05\text{‰}$ ), from the anomalous sample SMi-87, may reflect some devolatilization during regional metamorphism.

### 6.2. The Sierra Grande belt

The samples from this area are often dolomitic and only seven, from three specific sectors, were considered suitable for analysis (Fig. 2). These are calcite marbles with contents of Ca = 31.92–40.72 wt%, Mg = 0.01–0.507 wt%, Sr = 828–3513 ppm; Fe = 11–59 ppm and Mn = 0.35–8.71 ppm (most <1 ppm Mn) (Table 2). In all cases the Mn/Sr, Mg/Ca and Fe/Sr ratios and the IR values are low or very low, suggesting that the rocks did not undergo significant post-sedimentary alteration (Table 2, Fig. 6). Five samples yielded  $^{87}\text{Sr}/^{86}\text{Sr}$  ratios values between 0.70737 and 0.70740, similar to but slightly lower than those of the Sierra Chica belt, and two yielded 0.70836 and 0.70848 (Table 2, Fig. 6). C and O-isotope compositions of three samples ( $\delta^{13}\text{C}_{\text{PDB}} = +0.73$  to  $+3.2\text{‰}$ ;  $\delta^{18}\text{O}_{\text{PDB}} = -4.86$  to  $-9.14\text{‰}$ , Table 2) again suggest little post-sedimentary alteration of former marine limestones.

### 6.3. Other outcrops

Marbles from Cienaga del Coro were not considered because they are dolomitic. Four samples were analysed from the other sectors: two from Achiras and two from San Luis. They are calcite marbles with contents of Ca = 37.95–35.52 wt%; Mg = 0.08–0.77 wt%; Sr = 305–2106 ppm; Fe = 305–343 ppm and Mn = 0.2–126 ppm (Table 2). None of the samples yielded Mn/Sr, Mg/Ca and Fe/Sr ratios indicative of significant post-sedimentary changes. IR values range from 1.25 to 6.03 wt%, i.e., slightly higher than in the other two belts (Table 2 and Fig. 6). Three samples have  $^{87}\text{Sr}/^{86}\text{Sr}$  ratios of 0.70743 to 0.70764 and one gave 0.70786, mostly within the range of the less radiogenic group recognised in the other two belts. C and O-isotope composition of one sample ( $\delta^{13}\text{C}_{\text{PDB}} \sim +2.78\text{‰}$ ;  $\delta^{18}\text{O}_{\text{PDB}} \sim -7.91\text{‰}$ , Table 2) are also similar to those described before.

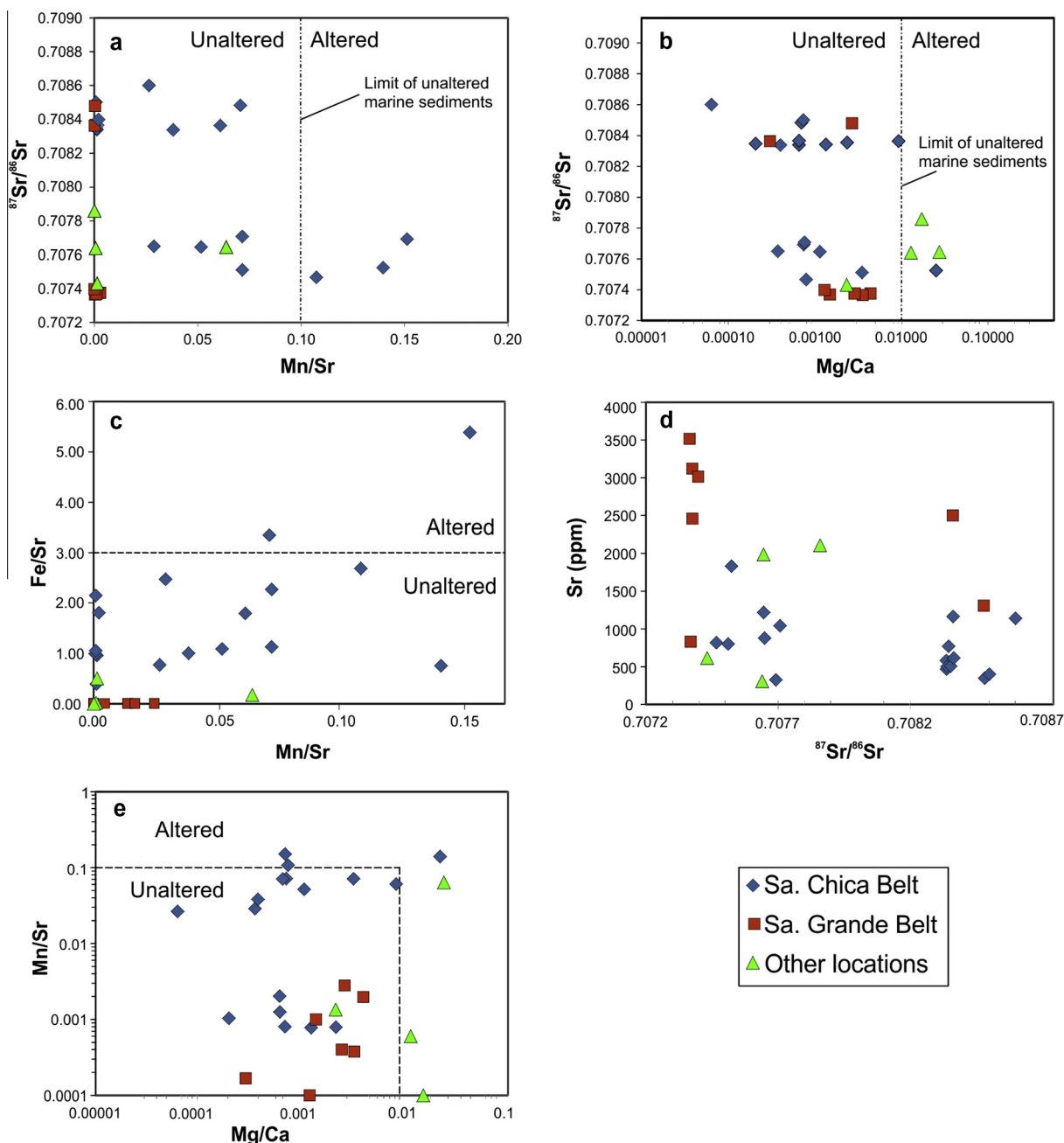


Fig. 6. Chemical screening plots of marbles from the Sierras de Córdoba showing the post-depositional alteration boundaries according to Melezhik et al. (2001).

## 7. U–Pb SHRIMP zircon geochronology

Fifty-six spots were analysed in sample LC-158 (Table 3). Two textural types of zircon were recognised (Fig. 7). The first consists of elongated grains (80–150  $\mu\text{m}$ ) often with a core showing oscillatory zoning and a discordant overgrowth with variable cathodo-luminescence (CL). The second group consists of equant grains (20–100  $\mu\text{m}$ ), sometimes internally simple with low CL and complex sector-zoning, or composite with a homogenous low-CL core and a low-CL zoned rim. The first group has high Th/U ratios (0.14–1.89) typical of igneous zircons and ages between ca. 700 and 1650 Ma; there is a notable peak at ca. 1190 Ma (range 1100–1250 Ma), and an older population with ages of ca. 1950–2060 Ma (Fig. 8). The second group shows typical high-grade metamorphic zoning (e.g., Harley et al., 2007), low Th/U ratios between 0.02 and 0.05 and ages between 514 and 535 Ma, i.e., early to mid-

dle Cambrian (Terreneuvian and Series 2, according to the 2015 IUGS chronostratigraphic chart). One spot with an unrealistic low age (ca. 300 Ma) was not considered. A weighted mean age for the second group is  $527 \pm 2$  Ma ( $n = 14$ ; MSWD = 2.2) (Fig. 8a). Rims were not analysed because of their small thickness.

## 8. Discussion

Recent compilations of Sr and C (and O-isotope in lesser degree) composition in Phanerozoic and Proterozoic seawater show trends that can be used to estimate the age of unfossiliferous marine carbonates assuming that they preserved original compositions unmodified by diagenesis and metamorphism (Veizer et al., 1999; Jacobsen and Kaufman, 1999; Montañez et al., 2000; Melezhik et al., 2001; Jiang et al., 2007; Prokoph et al., 2008; Halverson et al., 2010). The method is particularly useful for

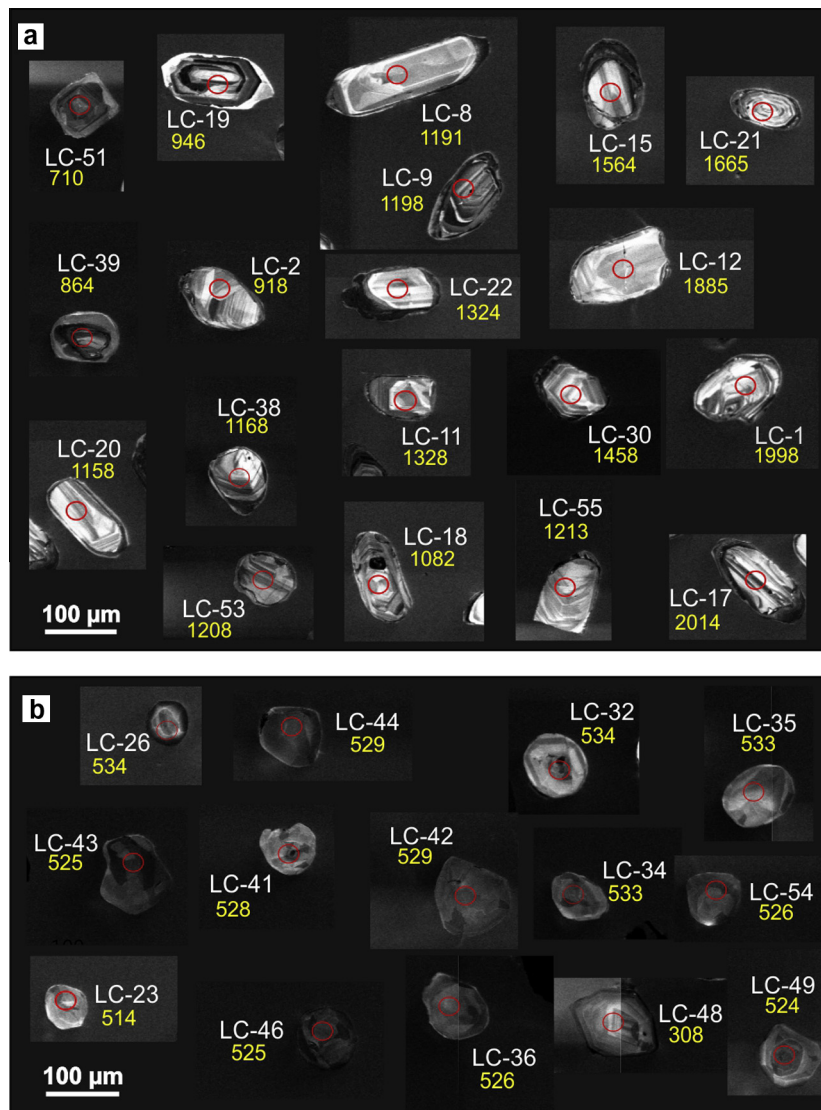


**Fig. 7.** Cathodoluminescence (CL) images of zircon grains from sample LC-158 showing location of analysed spots and age. (a) Detrital elongated igneous grains; (b) metamorphic grains. See text for details.

periods where the fossil evidence is scarce or absent, as is usually the case for Proterozoic rocks. The  $^{87}\text{Sr}/^{86}\text{Sr}$  ratio and the C-isotope composition are widely used, the first for dating (blind dating) and the second to infer paleoenvironmental conditions. The O-isotope composition however can be more easily modified through interaction with meteoric water and high-temperature percolating fluids (Fairchild et al., 1990). Despite the relative vulnerability of carbonates to diagenetic and metamorphic processes, they can often retain the original isotope compositions even under medium- to high-grade conditions (Brand and Veizer, 1980; Melezhik et al., 2001).

### 8.1. Geochemical evidence

The Mg content is very low in all the samples (<1 wt%), indicating that calcite is the only carbonate present or is the most abundant (Mg/Ca is in fact lower than 0.03 in all samples). Moreover, the content of impurities as estimated from the insoluble residue is generally less than 3 wt%, in many cases <1 wt% (Table 2). The main accessory minerals are quartz, phlogopite, opaque minerals, tremolite and diopside, along with others found at trace levels

(Table 1). The moderate to high contents of Sr (300–3500 ppm), the very low Rb values (<0.2 ppm), the  $^{87}\text{Sr}/^{86}\text{Sr}$  values, the Mg/Ca, Mn/Sr and Fe/Sr ratios, the low Mn contents and the C and O-isotope compositions all suggest that the rocks underwent minor post-sedimentary alteration and that protoliths were marine calcite and aragonite limestones. Therefore dating based on comparison of the  $^{87}\text{Sr}/^{86}\text{Sr}$  values with existing compilations should yield acceptable constraints on the ages of sedimentation. C-isotopes can help to better constrain the chronology.

The  $^{87}\text{Sr}/^{86}\text{Sr}$  values of the Sierra de Córdoba marbles fall between 0.70736 and 0.70786 (16 samples) and between 0.70834 and 0.70860 (12 samples). There is no clear geographical separation of the two groups; whilst the more radiogenic group appears to be predominant in the east and the less radiogenic in the west (Fig. 2) further sampling is needed to confirm this issue. Fig. 9a shows the compilation of  $^{87}\text{Sr}/^{86}\text{Sr}$  and C-isotope values of seawater for the late Proterozoic to the Cambrian/Ordovician boundary according to Halverson et al. (2010) and Kuznetsov et al. (2013). The less radiogenic group of  $^{87}\text{Sr}/^{86}\text{Sr}$  values is uniquely coincident with seawater composition at 620–635 Ma, i.e., early Ediacaran. We note that it has recently been



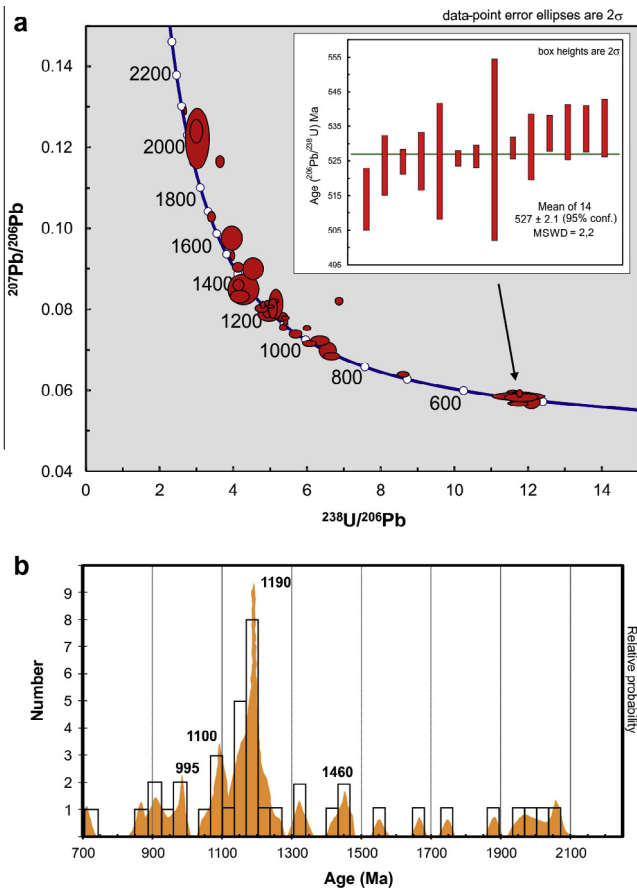


**Fig. 8.** U–Pb zircon results for migmatite gneiss LC-158. (a) Tera-Wasserburg diagram plotted without common Pb-correction (error ellipses are 68% confidence limits); (b) probability density plot of ages of pre-metamorphism detrital grains.

demonstrated that carbonates in the Bambui Group of the southern San Francisco craton with low  $^{87}\text{Sr}/^{86}\text{Sr}$  ratios of ca. 0.7075 were apparently laid down at  $\leq 570$  Ma (Paula-Santos et al., 2015). However, in that case, local morphotectonic conditions along the margin of the craton were thought to have modified the Sr-isotope composition of the sea, since sedimentation took place in a restricted foreland basin between the San Francisco craton and emerging chains of the Araçuáí orogen. The more radiogenic  $^{87}\text{Sr}/^{86}\text{Sr}$  ratios of the second group in the Sierras de Córdoba are ambiguous and match the seawater compilation at three different ages: mid-Cambrian (ca. 515 Ma), Ediacaran/Cambrian boundary (ca. 545 Ma), and mid-Ediacaran (ca. 580 Ma).

From consideration of the C-isotopes alone, it could be suggested that the Sierras de Córdoba Metasedimentary Series represents a single period of deposition on one side or other of the Shuram-Wonoka excursion (Fig. 9a) – between ca. 600 and 550 Ma seawater  $\delta^{13}\text{C}_{\text{PDB}}$  were all negative, down to ca.  $-12\text{‰}$  (Melezhik et al., 2009) – i.e., either earlier Ediacaran or late Ediacaran/Cambrian. Nevertheless, using the Halverson et al., 2010 seawater trend, the  $\delta^{13}\text{C}_{\text{PDB}}$  values of the less radiogenic group of samples ( $\delta^{13}\text{C} = -1.05$  to  $+3.54\text{‰}$ ) are compatible with the early Ediacaran age obtained from the Sr; such a peak of  $\delta^{13}\text{C}$  values from slightly negative to positive is recognised between 610 and 630 Ma. An early Ediacaran age for the less radiogenic group of marbles is also compatible with the maximum age of sedimentation recorded by the youngest detrital zircon in sample LC-158 (# 51;  $710 \pm 11$  Ma).

For the second group, the  $\delta^{13}\text{C}_{\text{PDB}}$  values ( $\delta^{13}\text{C} = +0.73$  to  $+2.03\text{‰}$ ) are most compatible with the Ediacaran/Cambrian option, i.e., ca. 545 Ma. In this case the older, mid-Ediacaran, option can be

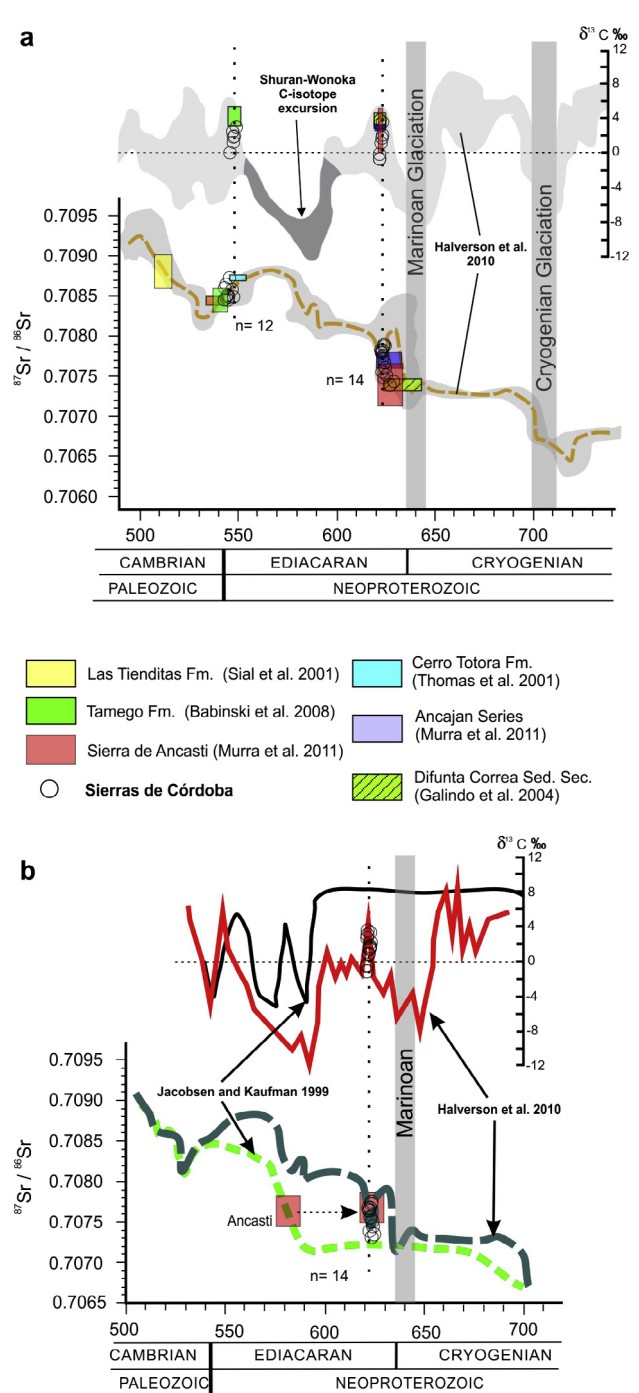


**Fig. 9.** (a)  $^{87}\text{Sr}/^{86}\text{Sr}$  ratios and  $\delta^{13}\text{C}_{\text{PDB}}$  composition of Neoproterozoic to the Early Palaeozoic seawater carbonates after compilation of Halverson et al. (2010). The Sierras de Córdoba marbles with  $^{87}\text{Sr}/^{86}\text{Sr}$  ratios of 0.7074–0.7077 suggest an Ediacaran age of sedimentation whilst  $^{87}\text{Sr}/^{86}\text{Sr}$  ratios of 0.7083–0.7086 suggest an early Cambrian age (see text for discussion). The  $\delta^{13}\text{C}_{\text{PDB}}$  values of Ediacaran marbles further constrain the proximity to the Marinoan glaciation age. (b) Updating of the Sierra de Ancasti early marble age by Murra et al. (2011) according to the recent isotope compilation of Halverson et al. (2010). (See above-mentioned references for further information.)

rejected as at this time  $\delta^{13}\text{C}$  values should be all negative (coincident with the Shuram-Wonoka excursion). Variations of  $\delta^{13}\text{C}$  have however been recorded in the mid Ediacaran between ca. 600 and 550 Ma (Verdel et al., 2011; An et al., 2015). However all the  $\delta^{13}\text{C}$  values found in the more radiogenic group of rocks of the Sierras de Córdoba Metasedimentary Series are slightly negative to

positive, never strongly negative. Thus we should have to invoke an intervening period of slightly negative to positive  $\delta^{13}\text{C}$  values during the Shuram–Wonoka period. This possibility remains true on the basis of C-isotope values only. However the Sr-isotope values are against this possibility because they are much higher than those typical of the Mid Ediacaran. We remind here that the Sr-isotope data obtained in this work are remarkably homogeneous and concentrated into two distinct ages on both sides of the Shuram–Wonoka event. The coincidence of the Sr-isotope composition with that of the C-isotope composition in our rocks makes our interpretation the more realistic. The middle Cambrian option is more difficult to reject on the basis of Sr- and C-isotope compositions alone, but the fact that the peak of regional metamorphism in the Sierras de Córdoba took place in the early Cambrian at 525–530 Ma (see below) argues in favour of the second option, i.e., sedimentation close to the Ediacaran/Cambrian boundary.

We propose that the two groups of marbles represent two different ages of sedimentation. The inference is that marbles in the Sierras de Córdoba are part of an original sedimentary succession including siliciclastic and marine limestones that probably extended in time from the early Ediacaran to near the Cambrian/Ediacaran boundary. The possibility of basin restrictions that could produce local isotope composition deviations relative to the open sea is difficult to disprove and therefore our stratigraphic interpretation remains open to question. However, recent paleogeographic models for deposition of the isotopically equivalent Ancajan – Difunta Correa metasedimentary sequences of the Western Sierras Pampeanas, based on detrital zircon ages and Hf-isotope compositions (see below), suggest that the sedimentary basin was an open platform along the margin of a large continental block (e.g., Rapela et al., 2016).

## 8.2. Stratigraphic correlations

Murra et al. (2011) obtained Sr- and C-isotope compositions for marbles from the sierras of Ancasti and Ancaján (Fig. 1) where they are abundant (and were long quarried). Two populations of Sr-isotope ratios were recognised (at ca. 0.7076 and ca. 0.7085) that were interpreted as evidence for sedimentation at ~570–590 Ma according to the compilation of seawater isotope composition for the late Neoproterozoic and the Cambrian available at that time (Jacobsen and Kaufman, 1999). In fact it is now clear that the two populations are indistinguishable from those found in marbles from the Sierras de Córdoba. Accordingly they are re-interpreted according to the trends of Fig. 9a as stratigraphically correlative with the two groups of marbles identified here.

In the Western Sierras Pampeanas, marbles in the Difunta Correa Sedimentary Sequence, Sierra de Pie de Palo (Galindo et al., 2004) and the Tambillo Unit, Sierra de Umango (Varela et al., 2001) have  $^{87}\text{Sr}/^{86}\text{Sr}$  ratios comparable with those of the Ediacaran group from the Sierras de Córdoba (mostly 0.7073–0.7075) with mostly positive  $\delta^{13}\text{C}$  values, albeit up to +12. In consequence the Sierras de Córdoba marbles and those west of it as far as the Andean Cordillera Frontal can probably be stratigraphically correlated.

Limestones of the Las Tienditas Formation, representing a subtidal–supratidal environment and contemporary with the upper levels of the Puncoviscana Formation (Omarini et al., 1999) have  $^{87}\text{Sr}/^{86}\text{Sr}$  ratios higher than those of the Sierras de Córdoba and Ancasti (Sial et al., 2001; López de Azarevich, 2010) suggesting a younger sedimentation age and/or post-sedimentary alteration as inferred from the high Mg/Ca and Mn/Sr relations. Ages younger than early Cambrian are also indicated by the Sr-isotope compositions of limestones in the Cauçete Group, Sierra de Pie de Palo (Galindo et al., 2004) and the Argentine Precordillera (Thomas et al., 2001).

Detailed comparison with carbonates of alleged Ediacaran age outside the realm of the early Cambrian Pampean orogenic belt is beyond the scope of this contribution but requires some comment. The Arroyo del Soldado Group is probably one of the most thoroughly studied such successions: isotope information including C, Sr, Nd and Cr, along with palaeontology and accurate lithological descriptions have been presented by Gaucher et al. (2009) and Frei et al. (2011, and references therein). These authors conclude that deposition was late Ediacaran, although some of the Sr-isotope data (e.g., the Polanco Formation) do not match the Halverson et al. (2010) or Kuznetsov et al. (2013) seawater curves for this age. In contrast, Aubet et al. (2012, 2014) conclude that the Arroyo del Soldado Group may be as old as 700 Ma; the cross-cutting Sobresaliente granite has recently been dated at  $585 \pm 2$  Ma (Oyhantçabal et al., 2012). Sánchez Bettucci et al. (2010) were also very critical of the proposed chronology, stratigraphy and tectonic setting of the Arroyo del Soldado Group. Further south along the margin of the Río de la Plata craton, Rapela et al. (2011) argue for a pre-580 Ma sedimentation of the Sierras Bayas Group on the basis of detrital zircon chronology. Sr-isotope composition data (Gómez Peral et al. (2007) were not chemically screened and show moderate Sr contents (<500 ppm) and high Mg/Ca and Mn/Sr ratios, suggesting post-depositional alteration. Further comparison with the Sierras de Córdoba marbles would seem to be premature.

## 8.3. Constraints from U–Pb zircon ages

The younger group of U–Pb ages in sample LC-158, nine of which give a weighted mean age of  $527 \pm 2$  Ma, are from unzoned or complex sector-zoned zircons with low Th (<20 ppm) and Th/U (0.05 and less), strongly suggesting metamorphic growth. It is reasonable to assume that this closely approximates to the time of high-grade metamorphism, since it closely corresponds to the peak of the Pampean orogeny (Rapela et al., 1998b; Escayola et al., 2011). The single peak at 1190 Ma in the detrital zircon age pattern (Fig. 8b) implies middle to late Mesoproterozoic sources, but there are also some grains with ages of 1250–1660 Ma on one side of the main peak and 700–1050 Ma on the other. This pattern shows many similarities with those of detrital rocks from the Western Sierras Pampeanas interbedded with the Ediacaran marbles discussed above, i.e., the Difunta Correa Sedimentary Sequence and the Ancaján series (Cf. Fig. 7b from Rapela et al., 2016). Comparable patterns have also been reported for some rocks from north-western Argentina (e.g., sample PMXX2 in Adams et al., 2011). Most of the 770–1330 Ma zircon provenance can be explained by derivation from middle to late Mesoproterozoic basement exposed in the Western Sierras Pampeanas, where there are ca. 1070–1330 Ma igneous rocks as well as early Neoproterozoic A-type granitoids of ca. 770 and 850 Ma (Casquet et al., 2012; and references therein). However, zircon ages of ca. 1330–1560 Ma must reflect sources elsewhere: using Hf-isotope data for zircons of these ages, Rapela et al. (2016) argued in favour of sources in the Southern Granite–Rhyolite Province of southwestern Laurentia (1.3–1.5 Ga; Goodge et al., 2004, 2010). This idea was strengthened by Ramacciotti et al. (2015) with more complete detrital zircon evidence and Nd-isotope composition from the Difunta Correa Sedimentary Sequence, and they further invoked the Mazatzal Province of southwestern Laurentia as the source of a few grains at ca. 1.65 Ga. The scattered Paleoproterozoic detrital zircon ages of ca. 1950–2060 Ma in sample LC-158 were not recorded in either of these studies and their source is unknown.

The detrital zircon age pattern of Fig. 8b differs from that of the pre-Pampean Puncoviscana Formation of northwestern Argentina (defined as above) and equivalents of northern Sierra Chica and Sierra Norte de Córdoba (Adams et al., 2008, 2011; Escayola

et al., 2007; Rapela et al., 2007, 2016). There the pattern is strongly bimodal with peaks at ca. 600 and ca. 1000 Ma, with the youngest detrital zircons at 555–570 Ma; interbedded tuffs in the upper part of the series are ca. 537 Ma (Escayola et al., 2011). This pattern is indicative of regional sources in SW Gondwana (e.g., Rapela et al., 2016 and references therein; Kristoffersen et al., 2016).

#### 8.4. Tectonic implications

Marbles in the Sierras de Córdoba were laid down between the early Ediacaran and the very early Cambrian, apparently in two separate episodes, and are interbedded with siliciclastic rocks with a detrital zircon pattern similar to those of other marble-bearing series to the west (Ancaján series and the Difunta Correa Sedimentary Sequence in the Western Sierras Pampeanas). They differ in these respects from the Puncoviscana Formation and the Las Tien-ditas limestones, strengthening the idea that the Sierras de Córdoba Metasedimentary Series are unrelated to them. Instead they appear to be an extension of the marble-bearing series in the west, implying that the Grenvillian basement of the Western Sierras Pampeanas probably extended beneath them as well and that a tectonic contact must exist somewhere between the latter area and the northern Sierra Chica and Sierra Grande, where the metasedimentary Puncoviscana Formation is widespread (Casquet et al., 2014). The Sierras de Córdoba Metasedimentary Series was involved in the Pampean orogeny at middle crustal levels, in contrast to the sierras to the west (Ancaján, Ancasti and the Western Sierras Pampeanas) where no evidence of significant Pampean metamorphism has been recognised so far. Our work further shows that the Sierras de Córdoba Metasedimentary Series underwent high-grade metamorphism at  $527 \pm 2$  Ma (Fig. 8a); a previous U–Pb SHRIMP monazite age of  $522 \pm 8$  Ma for a gneiss sample (Rapela et al., 1998b) is within error of this. Metamorphism was accompanied by folding and ductile shearing in the middle crust. Marbles and meta-siliciclastic rocks of the Sierras de Córdoba were overprinted by major shear zones (e.g., Martino, 2003) that were folded and/or imbricated, resulting in repetition on a W–E cross-section. A dismembered mafic to ultramafic igneous complex is also located in the same shear zones (Bonalmi and Gigena, 1987). This complex has been interpreted as an ophiolitic remnant embracing crustal tracts with oceanic-ridge and probably back-arc chemistry that were tectonically emplaced in a suture (e.g., Ramos et al., 2000), although the age of the mafic–ultramafic complex remains poorly constrained. Our results are compatible with the existence of a strongly reworked suture in the Sierras de Córdoba separating the Ediacaran to early Cambrian cover sequence and its basement in the west from the metasedimentary Puncoviscana Formation in the east. The former sedimentary cover would have been part of the lower colliding plate, since Pampean magmatic rocks were emplaced in the Puncoviscana Formation (Rapela et al., 1998b). The Pampean orogeny concluded the amalgamation of SW Gondwana (Rapela et al., 2007).

The existence of the Puncoviscana Formation in the Sierra de Ancasti (Toselli et al., 2005; Rapela et al., 2007) separated from the Ancaján series in the eastern part of the mountain range by a strongly deformed zone of Famatinian age, opens the question of the extent of the Pampean suture west of Sierras de Córdoba.

#### 8.5. Paleogeographic hypothesis

Casquet et al. (2012) proposed that the Western Sierras Pampeanas Paleoproterozoic to Mesoproterozoic basement was part of a single large continental block (the MARA block) along the western margin of the Clymene/Puncoviscan ocean (Trindade et al., 2006; Rapela et al., 2016) in Neoproterozoic times. The block

was juxtaposed to Laurentia until the early Cambrian when the latter rifted away and the Iapetus Ocean opened. The marble-bearing Difunta Correa Sedimentary Sequence and the Ancaján Series were laid down on this western margin, which collided with the eastern margin during the Pampean orogeny after early Cambrian closure of the Clymene/Puncoviscana ocean. This interpretation has been recently strengthened with more geochronological and Hf-isotope data from detrital zircons (Ramacciotti et al., 2015; Rapela et al., 2016).

We suggest here that the Sierras de Córdoba Metasedimentary Series was laid down on the continental margin of MARA in a more external position than the Ancaján and the Difunta Correa series. Therefore, it was thoroughly involved in the Pampean collisional orogeny whilst the Ancaján and the Difunta Correa rocks remained in the external part of the orogen or in its foreland where penetrative deformation and metamorphism were minor or absent.

## 9. Conclusions

The Sierras de Córdoba Metasedimentary Series consists of marbles of early Ediacaran and early Cambrian age and metasiliciclastic rocks that underwent high-grade metamorphism between 525 and 530 Ma during the collisional Pampean orogeny.

The Sierras de Córdoba Metasedimentary Series can be correlated on the basis of Sr-isotope evidence from marbles and U–Pb detrital zircon geochronology with other marble-bearing metasedimentary series in several sierras to the west of Sierras de Córdoba (e.g., the Difunta Correa Sedimentary Sequence and the Ancaján Series). All were part of a former sedimentary cover to the hypothetical MARA block and were laid down on the western margin of the Clymene/Puncoviscan ocean. The Sierras de Córdoba Metasedimentary Series strongly differs (in terms of the age of limestones/marbles and detrital zircon patterns) from the Puncoviscana Formation equivalents of northern Sierra Chica and Sierra Norte and northwestern Argentina. The latter are best interpreted as laid down on the late Ediacaran to early Cambrian eastern margin of the same ocean, with sedimentary input from Gondwana.

The Sierras de Córdoba Series and the Puncoviscana Formation (and its equivalents) were probably juxtaposed during the Pampean orogeny along a complex suture zone that was further folded and/or imbricated at middle crust depths. The suture has been inferred from structural evidence and supposed ophiolite remnants (Ramos et al., 2000).

## Acknowledgements

Financial support for this paper was provided by Argentine public grants SECYT-UNC 2014/2015 05/I768, FONCYT PICT 2013-0472, CONICET PIP 0229 and Spanish grants CGL2009-07984 and GR58/08 UCM-Santander. We acknowledge Dr. F. Tornos (Centro de Astrobiología, Madrid) and Dr. C. Recio (Salamanca University) for the stable isotope work. Ms. B. Soutullo (UCM) helped with some of the XRD determinations. This contribution has benefited from comments from Drs. Eben Hodgin and Paulo Boggiani, and two anonymous reviewers who helped us to improve the manuscript.

## References

- Adams, C., Miller, H., Toselli, A.J., Griffin, W.L., 2008. The Puncoviscana Formation of northwest Argentina: U–Pb geochronology of detrital zircons and Rb–Sr metamorphic ages and their bearing on its stratigraphic age, sediment provenance and tectonic setting. *Neues Jb. Geol. Paläontol. Abh.* 247, 341–352.
- Adams, C.J., Miller, H., Aceñolaza, F.G., Toselli, A.J., Griffin, W.L., 2011. The Pacific Gondwana margin in the late Neoproterozoic–early Paleozoic: detrital zircon U–Pb ages from metasediments in northwest Argentina reveal their maximum age, provenance and tectonic setting. *Gondwana Res.* 19 (1), 71–83.



- An, Z., Jiang, G., Tong, J., Tian, L., Ye, Q., Song, H., Song, H., 2015. Stratigraphic position of the Ediacaran Miaohu biota and its constraints on the age of the upper Doushantuo  $\delta^{13}\text{C}$  anomaly in the Yangtze Gorges area, South China. *Precamb. Res.* 271, 243–253.
- Aubert, N., Pecoits, E., Bekker, A., Gingras, M., Zwingmann, H., Veroslavsky, G., de Santa Ana, H., Konhauser, K., 2012. Chemostratigraphic constraints on early Ediacaran carbonate ramp dynamics, Río de la Plata craton, Uruguay. *Gondwana Res.* 22 (3–4), 1073–1090.
- Aubert, N., Pecoits, E., Heaman, L., Veroslavsky, G., Gingras, M., Konhauser, K., 2014. Ediacaran in Uruguay: facts and controversies. *J. S. Am. Earth Sci.* 55, 43–57.
- Babinski, M., Boggiani, P.C., Fanning, M., Simon, C.M., Sial, A.N., 2008. U–Pb SHRIMP geochronology and isotope chemostratigraphy (C, O, Sr) of the Tamengo Formation, southern Paraguay belt, Brazil. In: South American Symposium on Isotope Geology, 6, San Carlos de Bariloche, Argentina. Proceedings, CD-ROM.
- Baldo, E.G., 1992. Estudio petrológico y geoquímico de las rocas ígneas y metamórficas entre Pampa de Olaen y Characato, extremo norte de las Sierras Grandes de Córdoba, Córdoba, República Argentina. PhD, School Newspaper of Exact, Physical and Natural Sciences, National University of Córdoba, 305 p. (unpublished).
- Baldo, E., Casquet, C., Galindo, C., 1996. El metamorfismo de la Sierra Chica de Córdoba (Sierras Pampeanas). *Argentina. Geocaceta* 19, 51–54.
- Baldo, E., Rapela, C.W., Pankhurst, R.J., Galindo, C., Casquet, C., Verdecchia, S., Murra, J., 2014. Geocronología de las Sierras de Córdoba: revisión y comentarios. In: Martino, R., Guereschi, A. (Eds.), *Relatorio del XIX Congreso Geológico Argentino: Geología y Recursos Naturales de la Provincia De Córdoba*, pp. 845–868.
- Bonalumi, A.A., Gigena, A.A., 1987. Relación entre las metamorfitas de alto grado y las rocas básicas y ultrabásicas en el Dpto. Calamuchita, Córdoba. *Rev. Asoc. Geol. Argent.* 42 (1–2), 73–81.
- Bonalumi, A., Escayola, M., Kraemer, P., Baldo E., Martino, R., 1999. Sierras Pampeanas (Córdoba, Santiago del Estero). In: Caminos, R. (Ed.), *A) Precámbrico-Paleozoico inferior de las Sierras de Córdoba. Geología Argentina. Instituto de Geología y Recursos Minerales, Buenos Aires, Anales* 29, 136–140.
- Brand, U., Veizer, J., 1980. Chemical diagenesis of a multicomponent carbonate system – 1: trace elements. *J. Sediment. Petrol.* 50 (4), 1219–1236.
- Burke, W.H., Denison, R.E., Hetherington, E.A., Koepnick, R.B., Nelson, H.F., Otto, J.B., 1982. Variation of seawater  $^{87}\text{Sr}/^{86}\text{Sr}$  throughout Phanerozoic time. *Geology* 10 (10), 516–519.
- Casquet, C., Rapela, C., Pankhurst, R., Galindo, C., Dahlquist, J., Baldo, E., Saavedra, J., González Casado, J., Fanning, M., 2004. Grenvillian massif-type anorthosites in the Sierras Pampeanas. *J. Geol. Soc.* 162, 9–12.
- Casquet, C., Pankhurst, R., Rapela, C., Galindo, C., Fanning, C., Chiaradia, M., Baldo, E., González-Casado, J., Dahlquist, J., 2008. The Mesoproterozoic Maz terrane in the Western Sierras Pampeanas, Argentina, equivalent to the Arequipa–Antofalla block of southern Peru? Implications for West Gondwana margin evolution. *Gondwana Res.* 13 (2), 163–175.
- Casquet, C., Rapela, C.W., Pankhurst, R.J., Baldo, E.G., Galindo, C., Fanning, C.M., Dahlquist, J.A., Saavedra, J., 2012. A history of Proterozoic terranes in southern South America: from Rodinia to Gondwana. *Geosci. Front.* 3 (2), 137–145.
- Casquet, C., Rapela, C.W., Baldo, E., Pankhurst, R., Galindo, C., Verdecchia, S., Murra, J., Dahlquist, J., 2014. The relationships between pre- and syn-Pampean orogeny metasedimentary rocks in the Eastern Sierras Pampeanas. In: *Gondwana 15 Symposium, Abstracts book*, 29 (<http://eprints.uncm.es/26351/>) Madrid, España (Spain).
- Costa, C., Gardini, C., Chiesa, J., Ortiz Suárez, A., Ojeda, G., Rivarola, D., Tognelli, G., Strasser, E., Carugno Durán, A., Morla, P., Guersstein, P., 2001. Hoja Geológica 3366-III, San Luis, provincias de San Luis y Mendoza. SEGEMAR, Boletín 293, in CD.
- Craig, H., 1957. Isotopic standards for carbon and oxygen and correction factors for mass-spectrometric analysis of carbon dioxide. *Geochim. Cosmochim. Acta* 12 (1–2), 133–149.
- Dahlquist, J.A., Pankhurst, R.J., Rapela, C.W., Galindo, C., Alasino, P., Fanning, C.M., Saavedra, J., Baldo, E., 2008. New SHRIMP U–Pb data from the Famatina Complex: constraining early–mid Ordovician Famatinian magmatism in the Sierras Pampeanas, Argentina. *Geol. Acta* 6 (4), 319–333.
- Derry, L.A., Keto, L.S., Jacobsen, S.B., Knoll, A.H., Swett, K., 1989. Strontium isotopic variations in Upper Proterozoic carbonates from Svalbard and East Greenland. *Geochim. Cosmochim. Acta* 53, 2331–2339.
- Derry, L.A., Kaufman, A.J., Jacobsen, S.B., 1992. Sedimentary cycling and environmental change in the Late Proterozoic: evidence from stable and radiogenic isotopes. *Geochim. Cosmochim. Acta* 56 (3), 1317–1329.
- Do Campo, M., Ribeiro Guevara, S., 2005. Provenance analysis and tectonic setting of late Neoproterozoic metasedimentary successions in NW Argentina. *J. S. Am. Earth Sci.* 19 (2), 143–153.
- Escayola, M.P., Pimentel, M.M., Armstrong, R., 2007. Neoproterozoic backarc basin: sensitive high-resolution ion microprobe U–Pb and Sm–Nd isotopic evidence from the Eastern Pampean Ranges, Argentina. *Geology* 35 (6), 495–498.
- Escayola, M.P., van Staal, C.R., Davis, W.J., 2011. The age and tectonic setting of the Puncoviscana Formation in northwestern Argentina: an accretionary complex related to early Cambrian closure of the Puncoviscana Ocean and accretion of the Arequipa–Antofalla block. *J. S. Am. Earth Sci.* 32 (4), 438–459.
- Fairchild, I., Marshall, J., Bertrand-Sarafati, J., 1990. Stratigraphic shifts in carbon isotopes from Proterozoic stromatolitic carbonates (Mauritania): influences of primary mineralogy and diagenesis. *Am. J. Sci.* 290-A, 46–79.
- Frei, R., Gaucher, C., Døssing, L.N., Sial, A.N., 2011. Chromium isotopes in carbonates – a tracer for climate change and for reconstructing the redox state of ancient seawater. *Earth Planet. Sci. Lett.* 312 (1–2), 114–125.
- Fuenlabrada, J.M., Galindo, C., 2001. Comportamiento de la relación  $^{87}\text{Sr}/^{86}\text{Sr}$  en disoluciones de carbonatos impuros en función de la concentración ácida y en disoluciones de sulfatos en función del tiempo. *Actas III Congreso Ibérico de Geología*, 591–595.
- Galindo, C., Casquet, C., Rapela, C., Pankhurst, R.J., Baldo, E., Saavedra, J., 2004. Sr, C and O isotope geochemistry and stratigraphy of Precambrian and lower Paleozoic carbonate sequences from the Western Sierras Pampeanas of Argentina: tectonic implications. *Precamb. Res.* 131, 55–71.
- Gaucher, C., Sial, A.N., Poiré, D., Gómez-Peral, L., Ferreira, V.P., Pimentel, M.M., 2009. Chemostratigraphy. Neoproterozoic–Cambrian evolution of the Río de la Plata Palaeocontinent. In: Gaucher, C., Sial, A.N., Halverson, G.P., Frimmel, H.E. (Eds.), *Neoproterozoic–Cambrian Tectonics, Global Change and Evolution: A Focus on Southwestern Gondwana. Developments in Precambrian Geology*, vol. 16. Elsevier, pp. 115–122.
- Gómez Peral, L.E., Poiré, D.G., Strauss, H., Zimmermann, U., 2007. Chemostratigraphy and diagenetic constraints on Neoproterozoic carbonate successions from the Sierras Bayas Group, Tandilia System, Argentina. *Chem. Geol.* 237 (1–2), 109–128.
- Goodge, J.W., Williams, I.S., Myrow, P., 2004. Provenance of Neoproterozoic and lower Paleozoic siliciclastic rocks of the central Ross orogen, Antarctica: detrital record of rift-, passive-, and active-margin sedimentation. *Geol. Soc. Am. Bull.* 116 (9.10), 1253–1279.
- Goodge, J.W., Fanning, C.M., Brecke, D.M., Licht, K.J., Palmer, E.F., 2010. Continuation of the Laurentian Grenville Province across the Ross Sea Margin of East Antarctica. *J. Geol.* 118, 601–619.
- Gordillo, C., 1984. Migmatitas cordieríticas de las Sierras de Córdoba; condiciones físicas de la migmatización. *Bol. Acad. Nac. Cienc.* 68, 3–40.
- Gordillo, C., Bonalumi, A., 1987. Termobarometría de la faja migmatítica de “La Puerta”, Departamento Cruz del Eje, Provincia de Córdoba. *Rev. Asoc. Geol. Argent.* 42 (3–4), 255–266.
- Gordillo, C., Lencinas, A., 1979. Sierras Pampeanas de Córdoba y San Luis. Segundo Simposio de Geología Regional Argentina. *Acad. Nac. Cienc., Córdoba I*, 577–650.
- Guereschi, A., Martino, R., 2002. Geotermobarometría de la paragénesis Qtz + Pl + Bt + Grt + Sil en gneises del sector centro-oriental de la sierra de Comechingones, Córdoba. *Rev. Asoc. Geol. Argent.* 57 (4), 365–375.
- Guereschi, A., Martino, R., 2003. Trayectoria textural de las metamorfitas del sector centro-oriental de la sierra de Comechingones, Córdoba. *Rev. Asoc. Geol. Argent.* 58 (1), 61–77.
- Halverson, G.P., Dudás, F.Ö., Maloof, A.S., Bowring, S.A., 2007. Evolution of  $^{87}\text{Sr}/^{86}\text{Sr}$  composition of Neoproterozoic seawater. *Palaeogeogr. Palaeoclimatol.* 256 (3–4), 103–129.
- Halverson, G.P., Wade, B.P., Hurtgen, M.T., Barovich, K.M., 2010. Neoproterozoic chemostratigraphy. *Precamb. Res.* 182 (4), 337–350.
- Harley, S.L., Kelly, N.M., Möller, A., 2007. Zircon behaviour and the thermal histories of mountain chains. *Elements* 3 (1), 25–30.
- Iannizzotto, N.F., Rapela, C.W., Baldo, E.G., 2011. Nuevos datos geocronológicos, geoquímicos e isotópicos del Batolito de Sierra Norte-Ambargasta en su sector más austral, Provincia de Córdoba. 18º Congreso Geológico Argentino, Actas del Simposio de Tectónica Pre-Andina (52), 190–191, Neuquén.
- Jacobsen, S.B., Kaufman, A.J., 1999. The Sr, C and O isotopic evolution of Neoproterozoic seawater. *Chem. Geol.* 161 (1–3), 37–57.
- Jiang, G., Kaufman, A., Christie-Blick, N., Zhang, S., Wu, H., 2007. Carbon isotope variability across the Ediacaran Yangtze platform in South China: implications for a large surface-to-deep ocean  $\delta^{13}\text{C}$  gradient. *Earth Planet. Sci. Lett.* 261 (1–2), 303–320.
- Kristoffersen, M., Andersen, T., Elburg, M.A., Watkeys, M.K., 2016. Detrital zircon in a supercontinental setting: locally derived and far-transported components in the Ordovician Natal Group, South Africa. *J. Geol. Soc.* 173 (1), 203–215.
- Kuznetsov, A.B., 1998. Evolution of Sr isotopic composition in late Riphean seawater: the Karatau Group carbonates, Southern Urals (Unpub. Ph.D. thesis), St. Petersburg, Institute of Precambrian Geology and Geochronology, Russian Academy of Sciences, Russia, p. 190 (in Russian).
- Kuznetsov, A.B., Ovchinnikova, G.V., Gorokhov, I.M., Letnikova, E.F., Kurova, O.K., Konstantinova, G.V., 2013. Age constraints on the Neoproterozoic Baikal Group from combined Sr isotopes and Pb–Pb dating of carbonates from the Baikal type section, southeastern Siberia. *J. Asian Earth Sci.* 62, 51–66.
- Letnikova, E.F., Kuznetsov, A.B., Vishnevskaya, I.A., Terleev, A.A., Konstantinova, G.V., 2011. The geochemical and isotope (Sr, C, O) characteristics of the Vendian–Cambrian carbonate deposits of the Azyr–Tal Ridge (Kuznetsk Alatau): chemostratigraphy and sedimentogenesis environments. *Russ. Geol. Geophys.* 52, 1154–1170.
- Lira, R., Sfragulla, J., 2014. El magmatismo Devónico–Carbonífero: El batolito de Achala y plutones menores al norte del cerro Champaquí. In: Martino, R., Guereschi, A. (Eds.), *Relatorio del XIX Congreso Geológico Argentino: Geología y Recursos Naturales de la Provincia de Córdoba*, pp. 293–347.
- López de Azarevich, V., Omarini, R., Santos, R., Azarevich, M., Sureda, R., 2010. Nuevos aportes isotópicos para secuencias carbonáticas del Precámbrico superior (Formación Las Tienditas) del NO de Argentina: su implicancia en la evolución de la Cuenca Puncoviscana. *Serie Correlación Geológica* 26, 27–48.
- Ludwig, K.R., 2003. Isoplot/Ex version 3.0: a geochronological toolkit for Microsoft Excel. Berkeley Geochronology Center Special Publication N° 4, 2455 Ridge Road, Berkeley CA 94709, USA.

- Martino, R., 2003. Las fajas de deformación dúctil de las Sierras Pampeanas de Córdoba: Una reseña general. *Rev. Asoc. Geol. Argent.* 58 (4), 549–571.
- McCrea, J.M., 1950. On the isotopic chemistry of carbonates and a paleotemperature scale. *J. Chem. Phys.* 18 (6), 849–857.
- Melezhik, V.A., Gorokhov, I.M., Fallick, A.E., Gjelle, S., 2001. Strontium and carbon isotope geochemistry applied to dating of carbonate sedimentation: an example from high-grade rocks of the Norwegian Caledonides. *Precamb. Res.* 108 (3–4), 267–292.
- Melezhik, V., Pokrovsky, B., Fallick, A., Kuznetsov, A., Bujakaite, M., 2009. Constraints on  $^{87}\text{Sr}/^{86}\text{Sr}$  of Late Ediacaran seawater: insight from Siberian high-Sr limestones. *J. Geol. Soc. Lond.* 166, 183–191.
- Montañez, I., Osleger, D., Banner, J., Mack, L., Musgrove, M., 2000. Evolution of the Sr and C isotope composition of Cambrian oceans. *Geol. Soc. Am. Today* 10 (5), 1–5.
- Montero, P., Haissen, F., El Archi, A., Rjmati, E., Bea, F., 2014. Timing of Archean crust formation and cratonization in the Awasard-Tichla zone of the NW Reguibat Rise, West African Craton: a SHRIMP, Nd–Sr isotopes, and geochemical reconnaissance study. *Precamb. Res.* 242, 112–137.
- Murra, J.A., Baldo, E.G., Galindo, C., Casquet, C., Pankhurst, R.J., Rapela, C.W., Dahlquist, J., 2011. Sr, C and O isotope composition of marbles from the Sierra de Ancasti, Eastern Sierras Pampeanas, Argentina: age and constraints for the Neoproterozoic–Lower Paleozoic evolution of the proto-Gondwana margin. *Geol. Acta* 9, 79–92.
- Omarini, R., Sureda, R., Götze, H., Seilacher, A., Pflüger, F., 1999. Puncoviscana folded belt in northwestern Argentina: testimony of Late Proterozoic Rodinia fragmentation and pre-Gondwana collisional episodes. *Int. J. Earth Sci.* 88 (1), 76–97.
- Oyhantcábal, P., Wagner-Eimer, M., Wemmer, K., Schulz, B., Frei, R., Siegesmund, S., 2012. Paleo- and Neoproterozoic magmatic and tectonometamorphic evolution of the Isla Cristalina de Rivera (Nico Pérez Terrane, Uruguay). *Int. J. Earth Sci. (Geol. Rundsch.)* 101 (7), 1745–1762.
- Pankhurst, R.J., Rapela, C.W., 1998. The Proto-Andean margin of Gondwana: an introduction. In: Pankhurst, R.J., Rapela, C.W. (Eds.), *The Proto-Andean Margin of Gondwana*. Geological Society, London, Special Publications 142, pp. 1–9.
- Pankhurst, R.J., Rapela, C.W., Saavedra, J., Baldo, E., Dahlquist, J., Pascua, I., Fanning, C.M., 1998. The Famatinian magmatic arc in the central Sierras Pampeanas: an Early to Mid-Ordovician continental arc on the Gondwana margin. In: Pankhurst, R.J., Rapela, C.W. (Eds.), *The Proto-Andean Margin of Gondwana*. Geological Society, London, pp. 343–367. <http://dx.doi.org/10.1144/GSL.SP.1998.142.01.17>, Special Publications 142.
- Paula-Santos, G.M., Babinski, M., Kuchenbecker, M., Caetano-Filho, S., Trindade, R.I., Pedrosa-Soares, A.C., 2015. New evidence of an Ediacaran age for the Bambuí Group in southern São Francisco craton (eastern Brazil) from zircon U–Pb data and isotope chemostratigraphy. *Gondwana Res.* 28 (2), 702–720.
- Prokoph, A., Shields, G., Veizer, J., 2008. Compilation and time-series analysis of a marine carbonate  $\delta^{18}\text{O}$ ,  $\delta^{13}\text{C}$ ,  $^{87}\text{Sr}/^{86}\text{Sr}$  and  $\delta^{34}\text{S}$  database through Earth history. *Earth Sci. Rev.* 87 (3–4), 113–133.
- Ramacciotti, C.D., Baldo, E.G., Casquet, C., 2015. U–Pb SHRIMP detrital zircon ages from the Neoproterozoic Difuntosa Correa Metasedimentary Sequence (Western Sierras Pampeanas, Argentina): provenance and paleogeographic implications. *Precamb. Res.* 270, 39–49.
- Ramos, V., Escayola, M., Mutti, D. y Vujovich, G., 2000. Proterozoic-early Paleozoic ophiolites in the Andean basement of southern South America. In: Dilek, Y., Moores, E., Elthon, D. y Nicolas, A. (Eds.), *Ophiolites and Oceanic Crust: New Insights from Field Studies and Ocean Drilling Program*. Geological Society of America, Special paper, 349, pp. 331–349.
- Ramos, V.A., Vujovich, G., Martino, R., Otamendi, J., 2010. Pampia: a large cratonic block missing in the Rodinia supercontinent. *J. Geodyn.* 50 (3–4), 243–255.
- Rapela, C., Pankhurst, R., Casquet, C., Baldo, E., Saavedra, J., Galindo, C., 1998a. Early evolution of the Proto-Andean margin of South America. *Geology* 26 (8), 707–710.
- Rapela, C.W., Pankhurst, R.J., Casquet, C., Baldo, E., Saavedra, J., Galindo, C., Fanning, C.M., 1998. The Pampean orogeny of the southern proto-Andes: Cambrian continental collision in the Sierras de Córdoba. In: Pankhurst, R.J., Rapela, C.W. (Eds.), *The Proto-Andean Margin of Gondwana*. Geological Society, of London, Special Publication 142, pp. 181–217.
- Rapela, C.W., Casquet, C., Baldo, E., Dahlquist, J., Pankhurst, R., Galindo, C., Saavedra, J., 2001. Las Orogénes del Paleozoico Inferior en el margen proto-andino de América del Sur, Sierras Pampeanas, Argentina. *J. Iberian Geol.* 27, 23–41.
- Rapela, C.W., Baldo, E.G., Pankhurst, R.J., Saavedra, J., 2002. Cordierite and leucogranite formation during emplacement of highly peraluminous magma: the El Pilón Granite Complex (Sierras Pampeanas, Argentina). *J. Petrol.* 43 (6), 1003–1028.
- Rapela, C.W., Pankhurst, R., Casquet, C., Fanning, C., Baldo, E., González-Casado, J., Galindo, C., Dahlquist, J., 2007. The Río de la Plata craton and the assembly of SW Gondwana. *Earth Sci. Rev.* 83 (1–2), 49–82.
- Rapela, C.W., Pankhurst, R.J., Casquet, C., Baldo, E., Galindo, C., Fanning, C.M., Dahlquist, J., 2010. The Western Sierras Pampeanas: protracted Grenville-age history (1330–1030 Ma) of intra-oceanic arcs, subduction-accretion at continental-edge and AMCG intraplate magmatism. *J. S. Am. Earth Sci.* 29, 105–127.
- Rapela, C.W., Fanning, C.M., Casquet, C., Pankhurst, R.J., Spalletti, L., Poiré, D., Baldo, E.G., 2011. The Río de la Plata craton and the adjoining Pan-African/brasiliano terranes: their origins and incorporation into south-west Gondwana. *Gondwana Res.* 20 (4), 673–690.
- Rapela, C.W., Verdecchia, S.O., Casquet, C., Pankhurst, R.J., Baldo, E., Galindo, C., Murra, J.A., Dahlquist, J.A., Fanning, M., 2016. Identifying Laurentian and SW Gondwana sources in the Neoproterozoic to early Paleozoic metasedimentary rocks of the Sierras Pampeanas: paleogeographic and tectonic implications. *Gondwana Res.* 32, 193–212.
- Rasband, W.S., ImageJ, U. S. National Institutes of Health, Bethesda, Maryland, USA, <http://imagej.nih.gov/ij/>, 1997–2015.
- Sánchez Bettucci, L., Masquelin, E., Peel, E., Oyhantcábal, P., Muzio, R., Ledesma, J.J., Preciozzi, F., 2010. Comment on “Provenance of the Arroyo del Soldado Group (Ediacaran to Cambrian, Uruguay): implications for the palaeogeographic evolution of southwestern Gondwana” by Blanco et al. [*Precambrian Res.* 171 (2009) 57–73]. *Precamb. Res.* 180 (3–4), 328–333.
- Schwartz, J.J., Gromet, L.P., 2004. Provenance of Late Proterozoic–early Cambrian basin, Sierras de Córdoba, Argentina. *Precamb. Res.* 129 (1–2), 1–21.
- Schwartz, J.J., Gromet, L.P., Miro, R., 2008. Timing and duration of the calc-alkaline arc of the Pampean orogeny: implications for the Late Neoproterozoic to Cambrian evolution of Western Gondwana. *J. Geol.* 116 (1), 39–61.
- Sial, A.N., Ferreira, V.P., Aceñolaza, F.G., Pimentel, M.M., Parada, M.A., Alonso, R.N., 2001. C and Sr isotopic evolution of carbonate sequences in NW Argentina: implications for a probable Precambrian–Cambrian transition. *Carbonates Evaporites* 16 (2), 141–152.
- Sims, J., Ireland, T., Camacho, A., Lyons, P., Pieters, P., Skirrow, R., Stuart-Smith, P., Miró, R., 1998. U–Pb, Th–Pb and Ar–Ar geochronology from the southern Sierras Pampeanas, Argentina: implications for the Paleozoic tectonic evolution of the western Gondwana margin. In: Pankhurst, R., Rapela, C. (Eds.), *The Proto-Andean Margin of Gondwana*. Geological Society, London, Special Publication 142, pp. 259–281.
- Steenken, A., Wemmer, K., Martino, R.D., López De Luchi, M.G., Guerreschi, A., Siegesmund, S., 2010. Post-Pampean cooling and the uplift of the Sierras Pampeanas in the west of Córdoba (Central Argentina). *N. Jb. Geol. Paläont. Abh.* 256 (2), 235–255.
- Thomas, W., Astini, R., Denison, R., 2001. Strontium isotopes, age, and tectonic setting of Cambrian Salinas along the rift and transform margins of the Argentine Precordillera and Southern Laurentia. *J. Geol.* 109 (2), 231–246.
- Toselli, A., Aceñolaza, F., Sial, A., Rossi, J., Ferreira, V., Alonso, R., 2005. Los carbonatos de la Formación Puncoviscana s.l.: correlación quimioestratigráfica e interpretación geológica. XVI Congreso Geológico Argentino 2 (Actas), 327–333.
- Toselli, A.J., Gaucher, C., Aceñolaza, G.F., Frei, R., Aceñolaza, F.G., Sial, A.N., Rossi, J.N., 2010. New  $^{87}\text{Sr}/^{86}\text{Sr}$  data on limestones of the Puncoviscana Formation and Sierras Pampeanas of Catamarca, Argentina. VII – South American Symposium on Isotope Geology (VII-SSAGI). Brasília. Publicación CD-SO440.
- Toselli, A.J., Aceñolaza, G.F., Miller, H., Adams, C., Aceñolaza, F.G., Rossi, J.N., 2012. Basin evolution of the margin of Gondwana at the Neoproterozoic/Cambrian transition: the Puncoviscana Formation of Northwest Argentina. *N. Jb. Geol. Paläont. Abh.* 265, 79–95.
- Trindade, R., D’Ágrella-Filho, M., Epof, I., Brito Neves, B., 2006. Paleomagnetism of early Cambrian Itabaiana mafic dikes (NE Brazil) and the final assembly of Gondwana. *Earth Planet. Sci. Lett.* 244 (1–2), 361–377.
- Varela, R., Valencio, S., Ramos, A., Sato, K., González, P., Panarello, H., Roverano, D., 2001. Isotopic strontium, carbon and oxygen study on Neoproterozoic marbles from Sierra de Umango, Andean foreland, Argentina. III South American Symposium on Isotope Geology, Extended Abstracts, 450–453, Pucón, Chile.
- Veizer, J., Ala, D., Azmy, K., Bruckschen, P., Buhl, D., Bruhn, F., Carden, G.A.F., Diener, A., Ebneth, S., Godderis, Y., Jasper, T., Korte, C., Pawellek, F., Podlaha, O.G., y Strauss, H., 1999.  $^{87}\text{Sr}/^{86}\text{Sr}$ ,  $\delta^{13}\text{C}$  and  $\delta^{18}\text{O}$  evolution of Phanerozoic seawater. *Chem. Geol.* 161 (1–3), 59–88.
- Verdel, C., Wernicke, B.P., Bowring, S.A., 2011. The Shuram and subsequent Ediacaran carbon isotope excursions from southwest Laurentia, and implications for environmental stability during the metazoan radiation. *Geol. Soc. Am. Bull.* 123 (7–8), 1539–1559.
- von Gosen, W., McClelland, W.C., Loske, W., Martínez, J.C., Prozzi, C., 2014. Geochronology of igneous rocks in the Sierra Norte de Córdoba (Argentina): implications for the Pampean evolution at the western Gondwana margin. *Lithosphere* 6 (4), 277–300.
- Vujovich, G., van Staal, C., Davis, W., 2004. Age constraints on the tectonic evolution and provenance of the Pie de Palo Complex, Cuyania Composite Terrane, and the Famatinian Orogeny in the Sierra de Pie de Palo, San Juan, Argentina. *Gondwana Res.* 7 (4), 1041–1056.
- Whitney, D.L., Evans, B.W., 2010. Abbreviations for names of rock-forming minerals. *Am. Mineral.* 95, 185–187.
- Williams, I.S., 1998. U–Th–Pb geochronology by ion microprobe. In: McKibben, M.A., Shanks, W.C., III, Ridley, W.I. (Eds.), *Applications of Microanalytical Techniques to Understanding Mineralizing Processes*. Reviews in Economic Geology, vol. 7, pp. 1–35.
- Zimmermann, U., 2005. Provenance studies of very low- to low-grade metasedimentary rocks of the Puncoviscana complex, northwest Argentina. In: Vaughan, A.P.M., Leat, P.T., Pankhurst, R.J. (Eds.), *Geological Society, London, Special Publications* 246, pp. 381–416.